Universiteit Leiden
The Netherlands

F-19-nanoparticles: platform for in vivo delivery of fluorinated biomaterials for F-19-MRI

Mali, A.; Kaijzel, E.L.; Lamb, H.J.; Cruz, L.J.

Citation
Mali, A., Kaijzel, E. L., Lamb, H. J., & Cruz, L. J. (2021). F-19-nanoparticles: platform for in vivo delivery of fluorinated biomaterials for F-19-MRI. *Journal Of Controlled Release*, *338*, 870-889. doi:10.1016/j.jconrel.2021.09.001

Version:	Publisher's Version
License:	Creative Commons CC BY 4.0 license
Downloaded from:	https://hdl.handle.net/1887/3277485

Note: To cite this publication please use the final published version (if applicable).

Journal of Controlled Release 338 (2021) 870–889

Contents lists available at ScienceDirect

Journal of Controlled Release

journal homepage: www.elsevier.com/locate/jconrel

^{19}F-nanoparticles: Platform for *in vivo* delivery of fluorinated biomaterials for ^{19}F-MRI

Alvja Mali [a], Eric L. Kaijzel [a], Hildo J. Lamb [b], Luis J. Cruz [a,*]

[a] Translational Nanobiomaterials and Imaging (TNI) Group, Department of Radiology, Leiden University Medical Center (LUMC), Albinusdreef 2, 2333 ZA Leiden, the Netherlands
[b] Department of Radiology, Leiden University Medical Center, Leiden, the Netherlands

ARTICLE INFO

Keywords:
Fluorine-19
^{19}F magnetic resonance imaging
Perfluocarbons
Nanoparticles
Nanoprobes

ABSTRACT

Fluorine-19 (^{19}F) magnetic resonance imaging (MRI) features one of the most investigated and innovative techniques for quantitative and unambiguous cell tracking, providing information for both localization and number of cells. Because of the relative insensitivity of the MRI technique, a high number of magnetically equivalent fluorine atoms are required to gain detectable signals. However, an increased amount of ^{19}F nuclei induces low solubility in aqueous solutions, making fluorine-based probes not suitable for *in vivo* imaging applications. In this context, nanoparticle-based platforms play a crucial role, since nanoparticles may carry a high payload of ^{19}F-based contrast agents into the relevant cells or tissues, increase the imaging agents biocompatibility, and provide a highly versatile platform. In this review, we present an overview of the ^{19}F-based nanoprobes for sensitive ^{19}F-MRI, focusing on the main nanotechnologies employed to date, such as fluorine and theranostic nanovectors, including their design and applications.

1. Introduction

Nowadays, non-invasive ^{1}H-MRI is considered as imaging technique of choice for obtaining physiological and anatomical information because of its three-dimensional imaging capability at high resolution and excellent inherent soft tissue contrast. Specifically, MRI techniques have been extensively investigated for their ability to detect, track and quantify cells *in vivo*, for studying specific cellular events, and most importantly for monitoring several treatment responses. Non-invasive ^{1}H MRI is based on the NMR (nuclear magnetic resonance) phenomenon, described during the first half of the 20th century. Lauterbur and Mansfield were the first scientist who discovered how to create images from NMR signals [1]. This method relies on nuclear spin alignment of some atoms, such as hydrogens, within the external magnetic field. Transverse radiofrequency (RF) pulses are then introduced, which disrupt proton magnetic alignments, exciting the nuclei to either lower or higher energy spin states. Once RF pulses are turned off, the nuclei realign with the magnetic field releasing their absorbed extra electromagnetic energy and emitting RF signals. This excitation influences both protons longitudinal (T_1) and transverse relaxation (T_2) times [2].

Despite the many advantages of ^{1}H-MRI, its low sensitivity led scientists to develop numerous contrast agents (CAs), which will be discussed below in details. CAs work typically by affecting the ^{1}H signal of the water near the tissue of concern, hence enhancing MRI signals. However, the development of a "second color" MRI method has helped overcome the several contrast agent-related drawbacks, such as the need for pre-scans and potential artifacts due to the localization ambiguity [3,4]. In this regard, ^{19}F-MRI strategies, in addition to ^{1}H MRI, have received particular attention. This is because ^{19}F atoms have additional advantages such as their absence in the human body and the linear correlation between ^{19}F concentration and MRI signal, upon which quantitative analyses are carried out. Nevertheless, high concentration ^{19}F-contrast agents may be required to obtain an adequate signal-to-noise ratio, thus resulting in strong cytotoxicity *in vivo*. Besides the increased number of ^{19}F atoms per molecule, other strategies employed to tackle MRI sensitivity include namely pulse sequences improvement or magnetic field strength enhancement [5–7].

Nanoparticle (NP)-based platforms, such as liposomes, dendrimers, inorganic and polymeric NPs, have always been appealing strategies to increase ^{19}F contrast agent biocompatibility, delivery efficiency, solubility, and signaling properties. Indeed, nanoparticles have interesting features because of their manageable and versatile structure and chemical properties: they afford a large core and shell composition variability.

* Corresponding author.
E-mail address: L.J.Cruz_Ricondo@lumc.nl (L.J. Cruz).

https://doi.org/10.1016/j.jconrel.2021.09.001
Received 24 May 2021; Received in revised form 1 September 2021; Accepted 2 September 2021
Available online 4 September 2021
0168-3659/© 2021 The Author(s). Published by Elsevier B.V. This is an open access article under the CC BY license (http://creativecommons.org/licenses/by/4.0/).

Table 1
Summary of the most commonly used contrast agents containing nanoprobes for MRI techniques.

Nanoprobe	Contrast agent class	Sensitivity	Toxicity	Main advantages	Main drawbacks
Gd^{3+}-based nanoparticles MnO nanoparticles	T_1/positive agent	++	+++	- Induces of enhanced contrast signal - Mn^{2+} is a natural cellular mineral	- Human Toxicity - Signal intensity loss at increased concentrations - Affects cell functionality
SPIO nanoparticles	T_2*/negative agent	+++	++	- FDA approved - High sensitivity	- Inaccurate cell quantification
^{19}F-based nanoparticles	Heteronuclear atom	+	+	- No background signals - Unambiguous detection - Cell quantification	- High amount of ^{19}F atoms required for imaging at high sensitivity

Despite the many advantages of using nanoparticles, some key issues, such as their rapid uptake by reticuloendothelial system (RES) cells, undermine their implementation for clinical application.

Indeed, NP toxicity problems arise when nanoparticles are transported by circulating blood to the liver, spleen or bone marrow by the RES [8]. Moreover, a further fundamental problem in nanomedicine is the surface opsonization of nanoparticles. Indeed, after administration, nanoparticles undergo serum protein binding, forging the well-known protein corona on the nanodroplets surface, which encourages the particles uptake by phagocytic cells. In this regard, nanoparticle surface coating with polyethylene glycol (PEG), known as PEGylation, has always been considered an optimal solution for improving pharmacokinetic profiles and decreasing immunogenicity of nanoparticle-based drug or CAs delivery [9,10].

This review aims to provide a state-of-the-art overview of several nanotechnologies employed in ^{19}F nanoprobes development for MRI purposes. We will mainly highlight how nanotechnologies are vital for using perfluorocarbons, and how they may carry an increased number of ^{19}F atoms into cells or tissues, which can be imaged by ^{19}F-MRI. We will discuss the currently extensively investigated dual Lanthanide-^{19}F nanoprobes employed to enhance MRI sensitivity. Fluoropolymers, copolymers and lipids are a further pioneering and promising class used in ^{19}F nanoprobes development. These synthesized fluorinated biomaterials may incorporate a large amount of ^{19}F atoms, specifically arranged to be magnetically equivalent and with a single spectral peak, thereby avoiding the potential chemical shift artifacts that occur in the MRI imaging. Moreover, their efficient fluorine segments mobility may result in suitable relaxation times [11].

2. MRI contrast agents categories

Despite the high anatomical resolution and excellent soft-tissue contrast of MRI techniques, many contrast agents have been developed and employed over years to enhance the visibility of specific anatomical and pathological details in the imaged tissue. Indeed, these exogenous compounds modify the relaxation rate of water protons, affecting MRI signals. The minimum contrast agent concentration to acquire images is typically micro- or milli-moles per voxel and it depends on how intensively the contrast agent affects the local NMR relaxation rate [3].

Using contrast agents to improve the contrast difference between normal and abnormal tissue implies a longer acquisition time since it is necessary to acquire images before and after their administration in order to avoid ambiguous localization of the contrast molecules *in vivo* [3,12]. Among available contrast agents, paramagnetic MR contrast agents such as Gadolinium (III) (Gd^{3+}) and Manganese (II) (Mn^{2+}) are positive contrast agents which shorten the T_1 signals of water proton spins, resulting in a faster signal decay and a brighter area in the acquired image.

Despite the overall performance of gadolinium as CA, studies have reported several limitations as well. For instance, Gd^{3+} – chelates are less phagocyted by cells, which could result advantageous for intravascular imaging, but not for cell tracking. Indeed, for the last objective high contrast agent concentrations are required, which may provoke increased cytotoxicity. Nanotechnologies play a pivotal role in order to address the key issue of hampered phagocytosis as several formulations (such as liposomes [13], micelles [14], polymer-coated Gd-oxide nanoparticles [15]) have been developed over the years to increase intracellular gadolinium concentrations which enhance contrast signaling capacity. Furthermore, linear Gd^{3+}-based contrast agents have been found to accumulate in the brain, namely in severe inflammation in rats sepsis model [16], and gadodiamide, a gadolinium-based contrast agent has also been associated with nephrogenic systemic fibrosis [17]. In this context, nanoparticles may be considered as a potential solution for circumventing these important concerns.

With regard to manganese oxide (MnO) particles, studies have reported that they affect cell functionality, such as cellular survival [18] and differentiation capacity [19]. Also in this case, nanotechnologies have been exploited to strengthen contrast agent biocompatibility, stability, and MRI relaxivity.

Next to the T_1-enhancing CAs, superparamagnetic iron oxide (SPIO) particles are termed "T_2 agents", since they mostly affect the T_2 spin-spin relaxation time, causing signal loss in the tissue of interest [20]. SPIO nanoparticles are considered the most frequently used contrast agents for cell tracking, since they provide the highest detection sensitivity [21]. They consist of a solid iron oxide core coated with hydrophilic materials, such as polymers or lipids. Moreover, SPIO nanoparticles may be formulated in several sizes: MPIO particles are the largest ones with a diameter of about 1 μm, superparamagnetic iron oxides (SPIOs) are about 50–100 nm, and lastly the ultrasmall SPIO (USPIO) particles are the smallest with a diameter of less than 50 nm. Despite the great sensitivity of the iron oxide particles, these nanoprobes have been reported to accumulate extracellularly making the labeled cells difficult to distinguish from the background [22]. Additionally, it is hard to carry out quantitative analyses, since MRI signals do not proportionally increase to iron-oxide particles concentrations [23].

To overcome the above-mentioned CA-related issues (Table 1), the most relevant and promising strategy taken into consideration is the development of a "second color" or "hot spot" imaging, which involves the use of heteronuclear atoms such as ^{13}C, ^{23}Na, ^{31}P or ^{19}F in parallel with ^{1}H-MRI images [3,12]. Unlike T_1 and T_2 CAs, for therapeutic cell tracking purposes direct detection is possible through the use of these nuclei, thus preventing the need for pre-scans and the risk of false positives.

Among heteronuclear atoms, ^{19}F has received particular attention because of its high gyromagnetic ratio (γ), which is very close to that of hydrogen (40.08 *vs* 42.58 MHz/ T of ^{1}H) and its high nuclear magnetic resonance sensitivity which is 83% of ^{1}H. Moreover, ^{19}F fluorine is the naturally abundant isotope of fluorine and is not radioactive [24]. ^{19}F-MRI only traces exogenous fluorinated materials enabling to specifically image the labeled cells; therefore, ^{1}H-MRI is simultaneously used to obtain anatomical information.

Pioneering ^{19}F-based imaging agents for MRI have gained an increasing interest in recent years [25,26]. By using these promising contrast agents, several limitations associated with iron-oxide labeling might be overcome, such as signal loss caused by iron oxide NP indirect

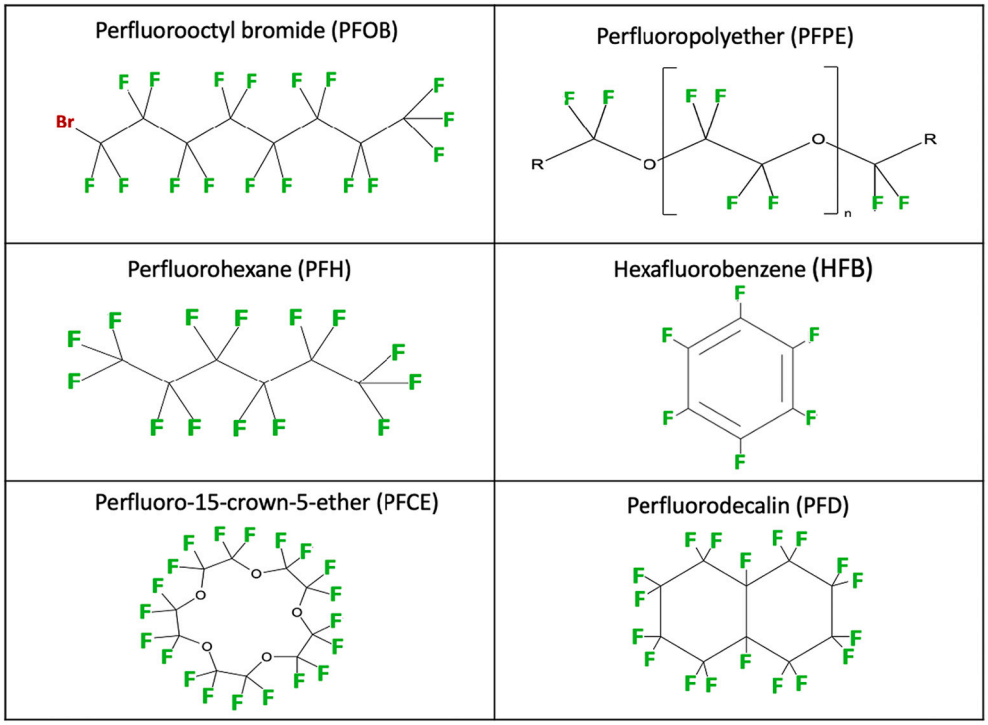

Fig. 1. Chemical structure of perfluorooctyl bromide (PFOB), perfluoropolyether (PFPEs), perfluorohexane (PFH), hexafluorobenzene (HFB), perfluoro-15-crown-5-ether (PFCE) and perfluorodecalin (PFD).

visualization, toxicity, and imprecise quantitative analyses.

Also, ^{19}F nuclei spins are directly detected and their sensitivity is proportional to the number of ^{19}F atoms per voxel.

Moreover, ^{19}F atoms are negligibly present in the body since the physiological concentration of detectable fluorine is below the detection limit. Hence, extrinsic ^{19}F-MRI signals may be merely detected without any background signal interference.

In the human body, bones and teeth have high concentrations of fluorine atoms. However, fluorine atoms are immobilized, leading to a very short T_2-relaxation time resulting in a background signal which is not detectable using conventional MRI machines [27].

As for iron-labeled cells, sensitivity for ^{19}F MRI-based cell tracking can be enhanced by increasing the amount of ^{19}F atoms internalized by cells [28]. Moreover, it has been demonstrated that many cell lines may be labeled with ^{19}F-based contrast agents and the efficiency of this process relies on cell type and size [29].

The main challenge in using ^{19}F-MRI techniques is related to delivery of fluorinated agents: a high payload of the relevant agent is needed in order to acquire images at high sensitivity. To address this problem, the number of fluorine atoms in MRI probes should be increased. However, it is crucial to take into consideration that increasing the number of ^{19}F atoms decreases solubility of the molecular probes.

3. Perfluorocarbons as tracers for ^{19}F-MRI

The most commonly used tracers for ^{19}F-MRI are perfluorocarbons (PFC), which are organic compounds in which all hydrogen atoms are replaced by fluorine, hence affording a high density of ^{19}F nuclei per molecule which increases contrast signal. Perfluorocarbons may be described as colorless liquids which are biologically inert, with a well-defined safety profile [30]. Furthermore, they are thermally, chemically, and oxidatively stable with a high vapor pressure and small surface tension. When fluorine binds to carbon, it gives rise to the strongest bond in organic chemistry, due to their remarkable electrostatic attraction, as a result of its high electronegativity [31].

Indeed, the C—F bond is highly polarized and it promotes either dipole-dipole or electrostatic interactions. When hydrogens are replaced by fluorine atoms, the polarization of the C—F bond drastically modifies the molecule's properties, including its geometric conformation [31]. A key limitation of fluorine-rich molecules is their "fluorous effect", which means their tendency to facilitate fluorine-fluorine interactions and form a separate phase, making them insoluble in both lipophilic and lipophobic solvents [30]. Fluorinated materials have peculiar biological properties due to their attractive chemical-physical properties, which drew the attention of scientists for use in medical applications [12].

Perfluoropolyethers (PFPEs) and perfluorocarbons (Fig. 1) showed an excessive accumulation in organs, in particular in spleen and liver, and it is well-recognized that these compounds are cleared through exhalation from the lungs after a prolonged period of retention in the liver [27,32].

With the aim to overcome several limitations, such as low water solubility, cytotoxicity, and clearance profile, and to obtain suitable *in vivo* formulations, several customizable delivery nanocarriers have been examined, for instance nanoemulsions and polymeric or lipid nanovectors.

In 2014, the first nanoemulsion-based formulation of PFCs was used in humans for ^{19}F-based cell imaging [29]. In this study, dendritic cells (DCs), after being labeled by the PFC-nanoemulsion, were intradermally administered and successfully imaged by ^{19}F-MRI during a phase-I trial for stage-4 colorectal cancer treatment with a DC-based vaccine. In contrast, iron oxide-based contrast agents showed a lower detection sensitivity of labeled cells in the first clinical application [33]. In addition to cell tracking, ^{19}F-MRI perfluorocarbon probes have been exploited for many applications, including oxygen transport, tumor imaging, hypoxia measurement detection, monitoring of enzymatic activity, blood flow measurement and the creation of blood vessels images [34,35]. *In vivo* tracking of therapeutic cells (*e.g.*, cell-based cancer immunotherapies) is classically performed by histological analyses or flow cytometry [16]. In this regard, perfluorocarbons revealed to be promising contrast agents to visualize immune cells and other cell types (*e.g.*, cancer cells and endothelial cells) *in vivo,* usually in parallel with the conventional ^{1}H-MRI, used for placing cells in their anatomical area.

Therefore, nanotechnologies play a crucial role in contrast agent delivery. Indeed, if adequately formulated, they may efficiently incorporate an extended label amount into cells without altering their functionalities while enabling cell imaging at high sensitivity for prolonged periods of time.

The most frequently used PFCs are perfluorooctyl bromide (PFOB) and perfluoro-15-crown-5-ether (PFCE). PFCE holds 20 magnetically equivalent fluorine atoms, thus providing a strong single resonance peak at −92.5 ppm, avoiding chemical shift artifacts when acquiring images and a correlated unambiguous identification of the tracer. By contrast, PFOB shows more than five ^{19}F NMR resonance peaks, and this characteristic is disadvantageous in terms of the imaging process and signal intensity [32,36]. Consequently, a higher concentration of the compounds is needed to create sufficient signal for MR imaging.

Despite these ideal PFCE properties of PFCE, it has a very long retention time within the body, which is therefore inappropriate for repetitive measurements. Indeed, PFCE clearance from the body requires more than 250 days [37]. The linear PFOB (also known as Perflubron) has a shorter blood half-time of about 12 days caused by the presence of the covalently bounded bromine which improves excretion from the body. Clearance of perfluorocarbons does not occur through metabolism since they are inert to biochemical degradation, but trough diffusion back into the bloodstream where they dissolve in plasma lipids, and then transported to the lungs where they are excreted through exhalation [36,37] . Furthermore, the presence of the terminal bromine in PFOB molecules makes it slightly lipophilic, hence, simplifying the production of stable nano-emulsions and promoting its passage through the cellular membrane.

The stable PFBO nanoemulsion has been proven to be safe in clinical trials as an oxygen carrier, for instance in patients undergoing cardiopulmonary bypass surgery [34]. The ^{19}F spin-lattice relaxation rate ($R_1 = 1/T_1$) of PFOB is linearly related to the partial oxygen pressure for a given magnetic field and temperature [38].

PFCE and PFOB T_1 and T_2 values are largely affected by tissue oxygenation, but their molecular structure may not undergo further functionalization processes without varying their MRI or biological performances; for instance, if PFCE is covalently modified, its cyclic symmetry will disappear thus provoking signal splitting and a decrease in signal intensity [12,39].

By contrast, the linear polymer PFPE T_1 value is less sensitive to oxygen tension alterations than PFOB, but PFPE may undergo chemical modifications. Furthermore, despite the high polydispersity of polymeric mixtures, the CF_2CF_2O repeated unit emits a major peak at −91.58 ppm [40].

Over time, other small, fluorinated molecules such as hexafluorobenzene (HFB), perfluorodecalin (PFD), and perfluorohexane (PFH) have been investigated.

HFB was found to show an excellent *in vivo* sensitivity to oxygen tension changes and fairly low sensitivity to temperature variation, leading to more accurate pO_2 determinations [41]. The optimal HFB sensitivity is also related to the fact that it exhibits a single resonance peak, since all the fluorine atoms are magnetically equivalent. Notwithstanding, Mignion et al. defined PFCE as a more appropriate probe than HFB for *in vivo* chronic muscle oxygenation (pO_2) measurements [42]. Moreover, PFN (perfluorononane) was been studied for ^{19}F MRI of the gastrointestinal tract, rendering it a non-toxic contrast agent [43].

PFD, which has a 9- day biological half-life, was tested as a probe for inflammation imaging, to address the challenging PFCE half-life. However, it showed a non-detectable MR signal in an inflammation mouse model [37].

4. Fluorinated molecules-encapsulated nanoprobes

Given the advantages of the ^{19}F probes, several types of ^{19}F-MRI nanotechnology platforms have been formulated for therapy and diagnosis of biological and pathological events *in vivo* and *in vitro* [44].

Due to their immiscibility with organic and inorganic solvents, perfluorocarbons need to be emulsified or incorporated into polymer or lipid nanoparticles. PFC-encapsulated NPs have a size under micrometer range, and they are usually formulated by vigorously mixing a water solvent and PFCs in the presence of a surfactant, and lastly by applying high pressure homogenization or sonication. Emulsifiers such as phospholipids and poloxamers reduce interfacial excess energy, preventing them from sticking together. Nevertheless, natural phospholipids from egg yolks, soybean, *etc.*, enable emulsions to be more stable and trigger less adverse reactions than poloxamers like Pluronic® [45,46].

4.1. Nanoemulsions

In 2005, Ahrens et al. [47] proposed the first successful nanoemulsion to track dendritic cells (DCs) by ^{19}F-MRI after *ex vivo* cell labeling. The presence of lecithin and safflower oil as emulsifiers maximized the fluorine content leading to enhanced MRI performance. Specifically, the ^{19}F agent consists of 40% *v*/v of PFCE, 2% lecithin and 2% safflower oil and water. Furthermore, the evaluation of potential PFPE nanoemulsion side effects based on cellular toxicity, metabolism, phenotype and proliferation, proved to be negligible. Afterwards, the biodistribution of the ^{19}F-labeled DCs was investigated by injecting the labeled cells *via* the tail vein and imaged by a 11.7 T ^{19}F MRI. The ^{19}F signal turned out to be enhanced in the liver and spleen and weak in the lungs.

The same group also formulated a similar PFPE nanoemulsion for T cells quantitative imaging analysis in order to carry out an in-depth investigation of the immunopathological process in nonobese diabetic mice [48]. Cells were labeled *ex vivo*, injected intravenously in mice, and lastly tracked by ^{19}F MRI combined simultaneously with ^{1}H-MRI, which is used to anatomically locate marked cells. In the study, no T cells activity impairment or cytotoxicity were noted when using poloxamers as emulsifier agents. Nonetheless, poloxamers have been found to activate the complement system, triggering an immune response [49].

Another interesting formulation to label phagocytic and non-phagocytic cells *ex vivo* has also been reported [40]. It consisted of a chemical modification of PFPEs. Their methyl esters react with the primary amine, located at one end of a lipophilic dye, thus forming the fluorescent blended PFPE amide (FBPA) contrast agent. The covalent conjugation of the fluorescent tag addresses the issue related to the dissimilar distribution of the dye and the contrast agent in tissue, which may occur when they are co-emulsified. The combined fluorescent-MRI cell monitoring technique yields unambiguous cell detection. Once synthetized, the PFPE mixture (FBPA and PFPE oxide) was emulsified in water using Pluronic F68 as emulsifier and PEI as a co-emulsifier and lastly microfluidized. The formulated nanoemulsion was employed to *ex vivo* label T cells, that were intraperitoneally injected and imaged by an 11.7 T MRI system and then by fluorescence microscopy. The ^{19}F images showed a localized accumulation of the labeled cells in lymph nodes (hepatic, mesenteric, and periaortic) and no signal was detected from the circulation since the concentration of labeled T cells was too low.

The stable and pioneering formulation was a source of inspiration for the synthesis of similar commercially available preparations known as Cell Sense. Some of these preparations are FDA-approved (*e.g.* CS-100, a PFPE-based contrast agent) and largely used for ^{19}F-MRI cell tracking [50]. For instance, the ^{19}F -nanoemulsion CS-100 will be employed in a first-in-human phase I trial, to track stromal vascular fraction (SVF) cells during treatment of radiation-induced fibrosis in breast cancer patients [51]. In the above-mentioned clinical study (ClinicalTrials.gov Identifier: NCT02035085), six female patients, who underwent breast lumpectomy and irradiation, will get liposuction, by means of which autologous SVF cell fraction will be isolated and labeled with the ^{19}F agent in the operating room, and lastly returned to the patient at the site of the breast grafting.

In another interesting phase-1 clinical study, the CS-100

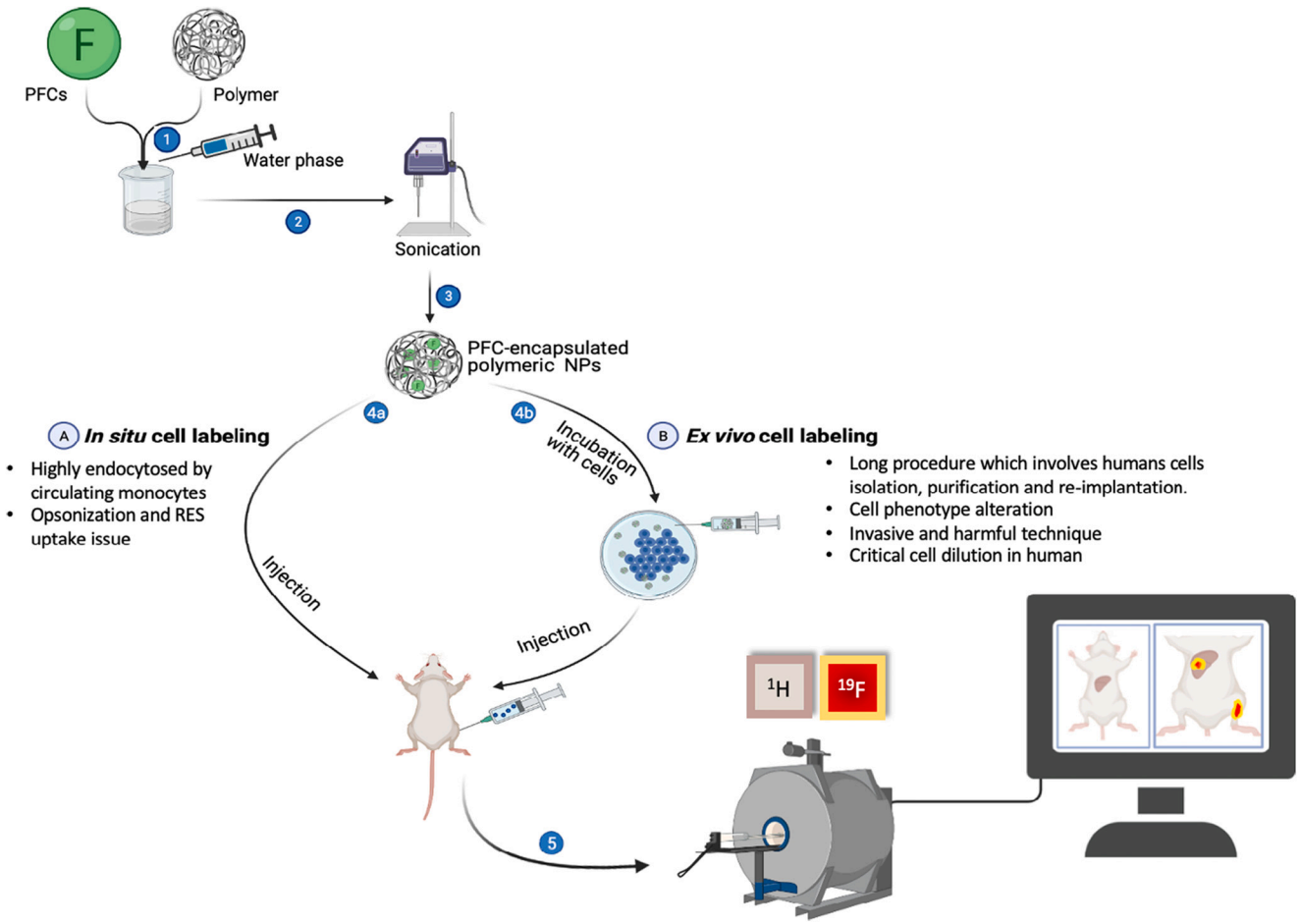

Fig. 2. Schematic drawing showing PFCs formulation into polymeric nanoparticles and their application for both *ex vivo* and *in situ* cell labeling and tracking, including the main drawbacks of the two strategies. Perfluorocarbons and polymers are dissolved in organic solvent, mixed with the water phase containing the emulsifying agent (1), and ultimately nanoparticles are formed by high pressure homogenization or sonication (2). PFC-encapsulated Nanoparticles (3) may either be directly injected *in vivo* (4a) for tracking cells by ^{19}F-MRI or incubated with isolated and purified cells (4b) and, in the final analysis, administered to mice, imaged using ^{19}F and ^{1}H-MRI in the same image session. The obtained images are overlaid so as to anatomically localize the nanoparticles.

nanoemulsion has been used to label and track peripheral blood mononuclear cells (PBMCs), which form the basis of an FDA-approved vaccine therapy for prostate cancer (ClinicalTrials.gov Identifier: NCT02921373). The long-term goal of the study is to successfully quantify immune cell migration to secondary lymphoid tissues and to tumors and correlate it to the therapeutic outcomes.

The main deficiency of the current approach for ^{19}F probe design is the limited capacity of nanoemulsions to be functionalized with targeting groups, antibodies, or additional fluorescent dyes for multimodal acquisition, since they are highly unstable in organic solvents by causing emulsion properties modification. The major instability problem is the well-known phenomenon called “Ostwald ripening”, in which small particles in solution dissolve and are deposited on large particles due to the poor affinity among surfactant, PFCs, and continuous aqueous phase [52,53].

Despite the encouraging data, it is essential to consider that the complete procedure to isolate, purify, incubate and re-implant cells requires time, and the phenotype of the cells may undergo some alterations. A further drawback of labeling cells *ex vivo* is the dilution of labeled cells by endogenous unlabeled cells [16].

To address these *ex vivo* labeling-related issues, several studies sought out to investigate label cells based on the interaction with nanoemulsions directly *in vivo* (Fig. 2). For instance, this method was employed to investigate local inflammation occurring after cerebral or cardiac ischemia. PFCE-nanoemulsions, injected intravenously, were both phagocytized by monocytes and macrophages cells that carried the payload of the relevant labels into the damaged area. However, the emulsion predominantly accumulated in the liver [54].

Nowadays, many scientists aim to functionalize and modify the structure of the contrast agent formulation to develop MRI probes with a specific role, such as selective targeting, pH evaluation, or metal ions concentration assessment.

In 2015, Temme et al. [55] synthetized α2-antiplasmin peptide ($\alpha2^{AP}$)-labeled perfluorocarbon nanoemulsions to target developing thrombi. α2-Antiplasmin is recognized as a selective marker as it is bound to fibrin by factor XIIIa at an early stage of thrombi development. They followed the same protocol as described by Flögel et al. [54] for nanoemulsion preparation and introduced α2-antiplasmin peptide into the formulation by mild sterol-based postinsertion technique (SPIT). Specifically, cholesterol-PEG_{200}-maleimide was synthetized, $\alpha2^{AP}$ cysteine residue was conjugated to a maleimide group, and lastly cholesterol-PEG- $\alpha2^{AP}$ was inserted into preformed nanoemulsions. By this means the cholesterol moiety was spontaneously embedded into the lecithin layer of PFCs. $\alpha2^{AP}$ and control-nanoemulsions were injected into mouse tail vein either before or after thrombus induction and were imaged by ^{19}F and ^{1}H-MRI at 9.4 T. In the study, almost no ^{19}F background signal was detected, and therefore an enhanced signal to noise ratio (SNR) (71 ± 22) was achieved when compared with the control-PFCs formulation. However, the SNR drastically declined 2 h after administration.

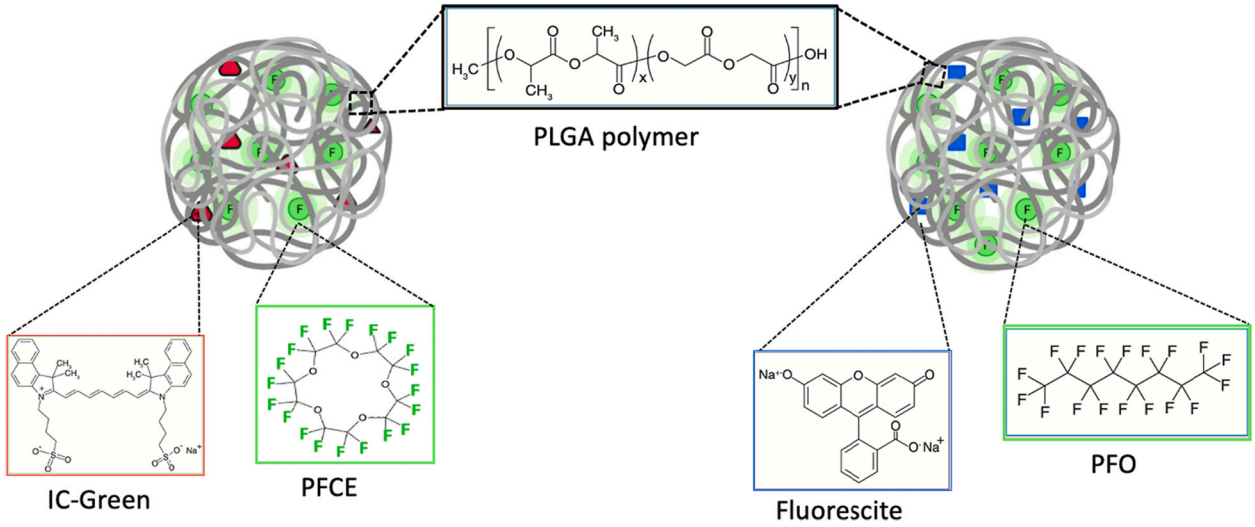

Fig. 3. (A) Nanoparticle's design; specifically, PFCE was co-encapsulated with IC-Green dye and PFO with Fluorescite, both in PLGA nanoparticles. (For interpretation of the references to color in this figure legend, the reader is referred to the web version of this article.)

Furthermore, several lipids, polymers and *co*-polymers have been investigated as coating to encapsulate and stabilize perfluorocarbons. Nanoparticle formulations have the advantage to be modified on their surface with the purpose of presenting targeting moieties and delivering several types of lipophilic and hydrophilic payloads, such as drugs or dyes for multimodality imaging [44].

4.2. Polymeric NPs

The FDA-approved Poly Lactic-*co*-Glycolic Acid (PLGA) is one of the most used co-polymers which has currently received particular attention both as a drug and contrast agent delivery vehicle. PLGA has been demonstrated to be easily degraded and metabolized in *in vivo* animal models, to carry a high hydrophobic payload, and to be modifiable for *in vivo* targeting. Moreover, the ability of PLGA coating, as a biodegradable polymeric shell, to enhance formulation stability along with mechanical strength, has been long reported as compared to traditional emulsions.

In 2010, Srinivas et al. [32] encapsulated several perfluorocarbons in PLGA-NPs by single and double emulsion techniques depending on the desired size. Afterwards, the feasibility of applying nanoparticle surface modifications, without altering the stability, was demonstrated by coating nanoparticles with DEAE-dextran and poly-L-lysine oligomers along with linking covalently an antibody to specifically target DCs. PFCE-entrapped PLGA nanoparticles with a diameter of about 200 nm were revealed to be suitable for ^{19}F-MRI in an *in vivo* animal model. Indeed, it gave the highest PFC encapsulation and showed a single resonance peak because of its symmetrical structure. Afterwards, nanoparticles or NPs-labeled cells were injected in the footpad of mice, and both were successfully detected by ^{19}F MRI. The signals decreased significantly over 7 days, because of the clearance of the nanoparticles from the injection site and no side effect have been observed in mice during that period.

Later on, an "optimized" version of the same protocol was applied to formulate nanoparticles for a contemporaneous monitoring of plasmacytoid and myeloid DCs by the gradient echo sequence technique [56]. PFCE or PFO- entrapped PLGA nanoparticles, with or without fluorescent dyes, were formulated with an average size of 180 nm and a regular spherical nature (Fig. 3). Cells, extracted from healthy volunteers' blood, were co-incubated with nanoparticles and magnetic resonance spectroscopy (MRS) was used to measure ^{19}F content per cell. Next, fluorescence imaging was carried out to reveal labeling effectiveness in both cell lines without requiring the use of transfection agents. Furthermore, nanoparticles did not interfere with cell functions and phenotype [56].

PLGA polymers were also exploited and investigated by Diou et al. [57] and Boissenot et al. [58] as perfluorocarbon-entrapped nanocapsules, as they developed PLGA-PEG nanocapsules encapsulating PFOB. PEG was introduced in the system developed by Diou et al. [57] in order to overcome the *in vivo* limitations due to the surface charge and consequently increase the plasma half-life. Using the emulsion-evaporation method, nanoparticles showed an average size of 120 nm, a smooth surface at SEM analysis and a very high encapsulation efficiency (85%). If compared to other similar studies [32], the encapsulation efficiency turned out to be ten-fold higher. As mentioned by Diou [57], this may be correlated to the use of the PVA as a surfactant instead of sodium cholate (SC). Stability studies revealed that after 120 h just about 11% of the nanocapsules had been destroyed. Afterwards, PLGA and PLGA-PEG nanocapsules were injected intravenously for tumor imaging. Both types of nanocapsules showed a significant accumulation in the liver and spleen after 4 h post-injection. However, the kinetics of the ^{19}F systems are different. Indeed, PLGA NCs concentration is high at the beginning and notably decreases after 7 h (from 5.3 ± 0.2% to 1.75 ± 0.2% in the spleen), indicating the progressive elimination of the nanosystem. On the other hand, PLGA-PEG NCs accumulate in the organs 7 h after administration.

This result proves the efficacy of PEGylation to increase half-life (13.6 min for PLGA and 23.9 min for PLGA-PEG capsules), allowing them to reach the tumor with a higher probability.

In general, nanocapsules are nanoparticles with an oily core in which drug and/or contrast agents can be dissolved, covered by a polymeric shell which controls the release profile of the core components. They are predominantly formulated by nanoprecipitation [59], but also by emulsion-evaporation [57].

Barnett et al. [60] developed alginate nanocapsules and demonstrated their capacity to encapsulate human islets and PFOB. Fluorinated capsules were monitored by ^{19}F-MRI and observed to increase insulin secretion, which is useful for a more efficient control of glucose levels in type 1 diabetes patients.

Nowadays, despite the extensive application of PLGA-PEG nanoparticles, little information is known about corona identity, cargo release mechanisms, and their interaction with biomolecules. So far, coating nanoparticles with PEG, an FDA-approved polymer, is the most commonly used technology to overcome nanoprobe opsonization and reticuloendothelial system uptake and retention. Specifically, the polymer decreases the absolute zeta potential value leading to a more neutral or negative surface charge, which in turn controls nanoparticles uptake

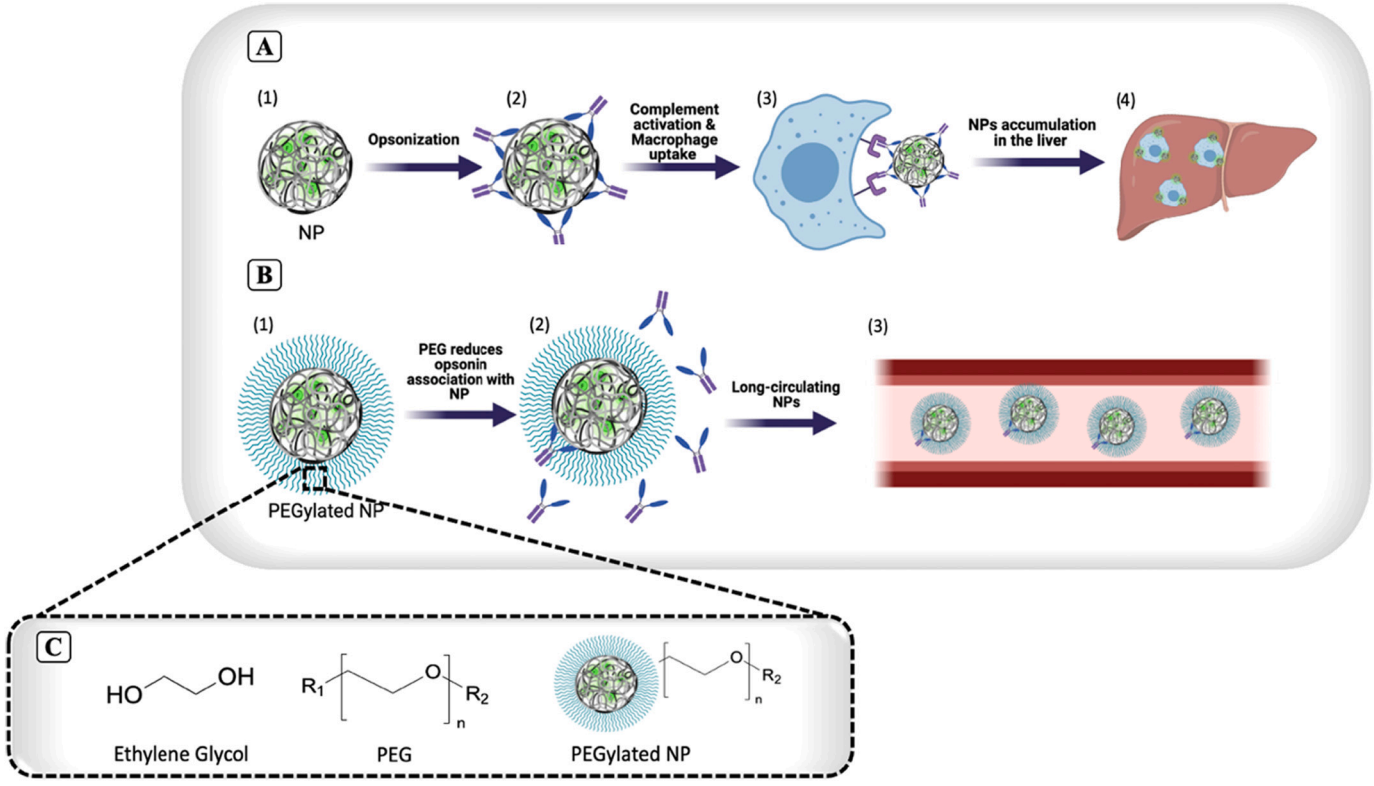

Fig. 4. PEGylation process discourages nanoparticles opsonization and reticuloendothelial system uptake. (A) Nanoparticles (A1) highly interact with opsonin proteins (A2) and are phagocyted by macrophages (A3) and carried to the liver (A4). (B) Pegylated nanoparticles (B1) prevent the opsonization process (B2), resulting in a reduced liver accumulation and a prolonged availability of nanoparticles for imaging and therapy (B3). (C) PEG polymers are composed of repeating ethylene glycol units. PEG contains both a linkage (R_1) and terminus group (R_2); the latter one interacting with the surrounding solvent.

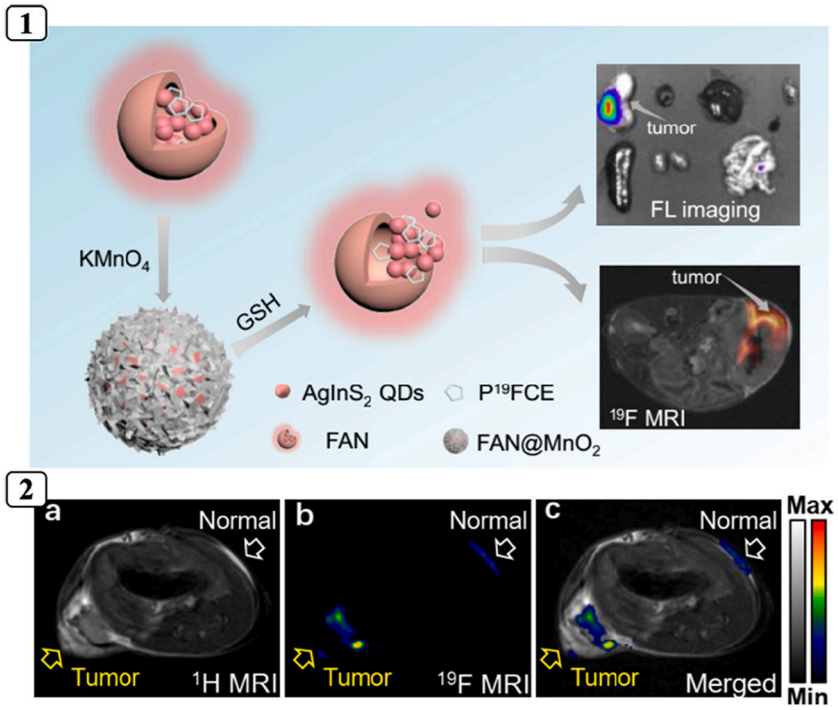

Fig. 5. (1) Illustrated representation of GSH-Activated FAN@MNO_2 Nanoprobes mechanism for ^{19}F-MRI/Fluorescence dual-modal tumor imaging. (2) *In vivo* ^{1}H-MRI (a), ^{19}F-MRI (b) and, merged images (c), 1 h after injection of the same amount of FAN@MNO_2 nanoprobes into tumor and normal tissue of the same mouse, respectively. Reprinted with permission from ref. [70]. *Copyright © 2020, American Chemical Society.*

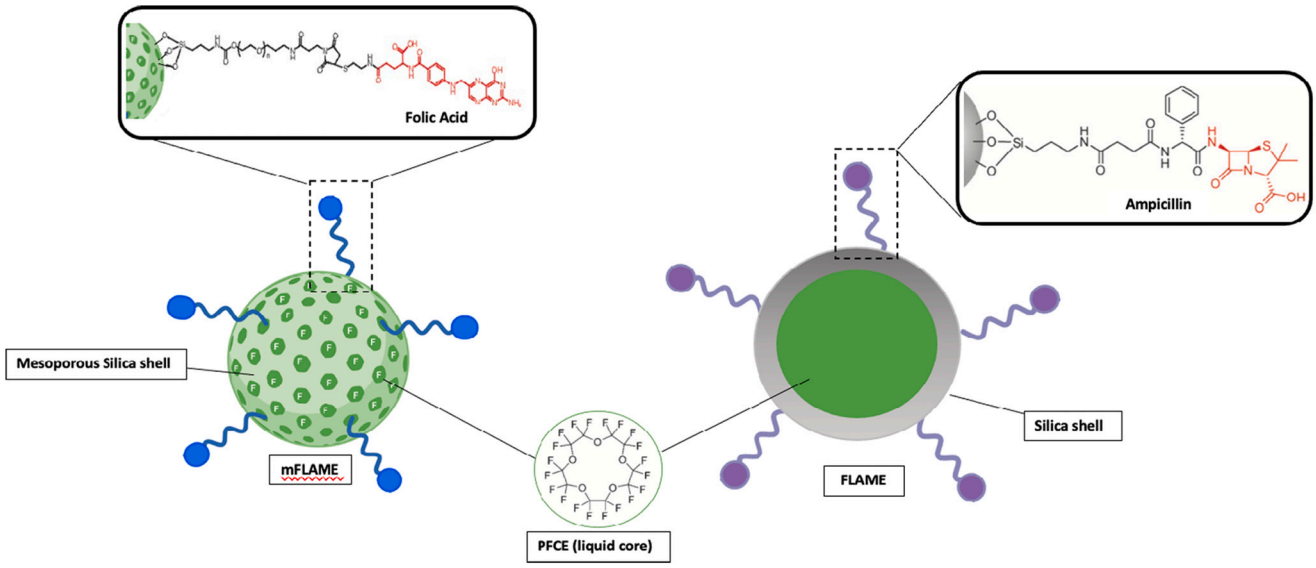

Fig. 6. Schematic design of FA-functionalized mFLAME (left) and ampicillin- FLAME (right), both composed by a PFCE liquid core and silica shell.

by the mononuclear phagocytosis cells, while minimizing the clearance by the RES. Basically, PEGylation helps to mask nanoparticles from degradation by the immune system, and consequently increasing nanoparticles circulation half-life to such an extent that it could be successfully used for imaging analysis or drug delivery [61,62] (Fig. 4). PEGylation may be obtained by different processes, such as physical adsorption, covalent grafting on performed nanoparticles or direct formulation using PEG-copolymers [63,64].

In this regard, Abstiens et al. [65] studied the correlation between the surface charge of the nanoparticles and serum proteins binding. They synthetized PLA-PEG copolymers with several end groups (methoxy, carboxy, and amine), and blended them with PLGA for nanoparticles preparation. Results showed that biomolecules highly interact with the positively charged NPs forming the so-called "hard corona" which causes a continuously cargo leaching from the core. By contrast, zwitterionic nanoparticles are less impaired than positive charged ones, since serum proteins may slightly interact with the nanoparticles by electrostatic or hydrophobic bounds. Doxil® and Abraxane® are some of the earliest FDA-approved PEG-NPs therapeutics [66,67].

Considering that, as above-mentioned, nanoemulsion surface droplets are hardly editable for ligand adding, PEG polymers have also been extensively exploited as nanoemulsion anchors to covalently bind the target. Sometimes, PEG polymers are part of the lipid mixture used to emulsify perfluorocarbons [68], and the target moiety is later attached to the pre-formed nanoemulsion. The target may be previously linked to the polymer, which in turn is bound to a phospholipid, which allows the nanoparticles' surface to be grafted [69].

In addition to the nanoparticles' instability drawback in human blood, another crucial aspect for clinical translation is their scale-up manufacturing process. Nowadays, scientists have particular interest in this last topic. For instance, Hoogendijk et al. [25] proposed a continuous-flow production of PFC-encapsulated PLGA nanoparticles by a microfluidic system. Moreover, in 2015, the same nanoparticles have been approved for a clinical trial and the studies are still ongoing (ClinicalTrials.gov Identifier: NCT02574377). PFCE-PLGA nanoparticles have been employed for labelling myeloid and plasmacytoid blood dendritic cells during the cell therapy of stage III melanoma patients.

In addition to PLGA, many other polymers and copolymers have been used to encapsulate perfluorocarbons and/or drugs. Zhang et al. [70] synthetized amphiphilic (oleylamine and 1-(3-aminopropyl) imidazole functionalized polysuccinimide) polymers for encapsulating both hydrophobic $AgInS_2$ QDs and perfluoro-15-crown-5-ether (PFCE) for dual-modality (Fluorescence and ^{19}F-MRI) tumor imaging. The resulting GSH-sensitive nanoparticles were further coated with an *in situ* formed manganese dioxide shell, which quenches and impairs the fluorescence and ^{19}F signals until elevated GSH concentrations (*e.g.,* in tumors), were able to break down the manganese shell in Mn^{2+}, recovering both signals. The nanoparticles' effectiveness was revealed by the T_2 value, which increased from 129 to 708 ms after incubation with GSH, and by the peak width which decreased from 33.5 to 14.3 Hz. In conclusion, these nanoparticles were found to be biocompatible *in vitro*, and the signals were strong enough to successfully conduct preclinical *in vivo* tumor imaging by ^{19}F-MRI (Fig. 5).

4.3. Liposomes

Liposomes are conventional nanocarriers, widely studied and used for perfluorocarbon delivery to address their hydrophobicity and concurrent lipophobicity. Liposomes are usually formulated by self-assembling of lipids, such as phospholipids, phosphatidylethanolamine, phosphatidylcholine, phosphatidylglycerol and cholesterol. They are structured so that liposomes show a hydrophobic lipid bilayer and a hydrophilic core. Moreover, the surface of liposomes may be functionalized in order to target specific cells, tissues, or organs. The critical point of liposomal nanocarriers is their delivery efficiency. In 2016, Wilhelm et al. [71] statistically analyzed the literature of the previous 10 years, and this study revealed that only 0.5% of the administered liposomes were supposed to reach the target. Lipid-based PFCE nanoemulsions used as ^{19}F-MRI contrast agents to track immune cells have been widely developed. For instance, Heleen et al. [72] developed PFCE-entrapped liposomes for DC tracking *via* ^{19}F-MRI. In this analysis, particles were intentionally formulated with an average diameter of 1 μm, notably larger if compared to other studies. Bigger size affords particular advantages regarding both the antigen-presentation and the ^{19}F-MRI of the particle-loaded cells. A layer-by-layer nanocarrier has been developed as well, to enhance the quantity of protein which may be loaded into the liposomes. Liposomes [72] consist of 63.7% DOTAP, 24.5% DOPE, 2% DSPE-PEG(2000) and 9.8% cholesterol. The obtained lipid film was then hydrated, emulsified with perfluorohexane or PFCE and lastly the system was electrostatically loaded with negatively charged ovalbumin, thus formulating theranostic nanoparticles. PFCE-incorporated liposomes showed an T_1 relaxation time of 1000 ± 100 and a T_2 of 350 ± 50 [ms]. The intracellular fluorine

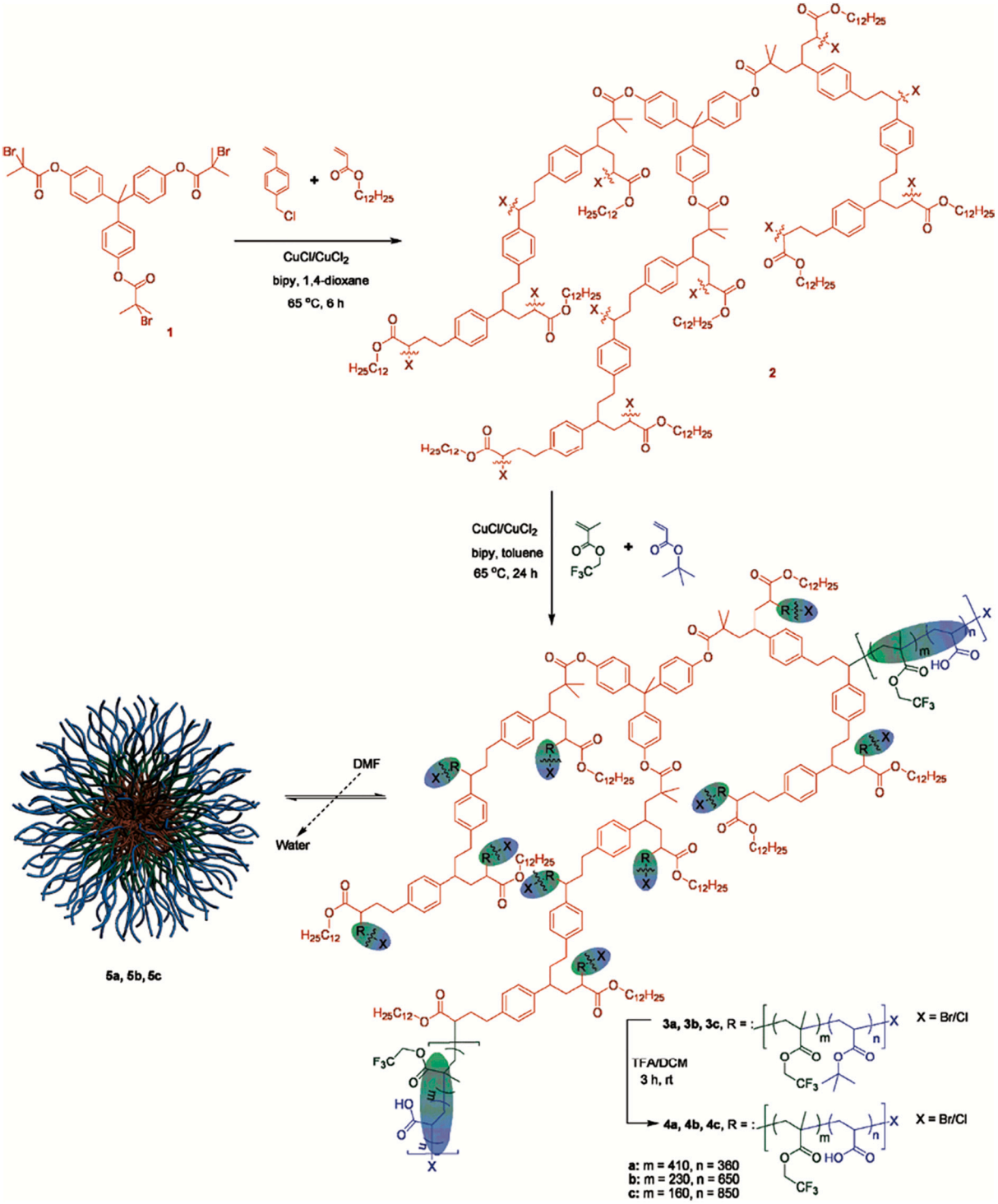

Fig. 7. Schematic illustration of hyperbranched fluoropolymers preparation and their self-assembly into micelles in aqueous solution. The dark red core units indicate the hydrophobic lauryl acrylate and *p*-chloromethylstyrene-based components, while the green and blue chains represent the trifluoroethyl methacrylate and acrylic acid copolymer branches extending from the hyperbranched core. Reprinted with permission from ref. [78]. *Copyright © 2008, American Chemical Society. (For interpretation of the references to color in this figure legend, the reader is referred to the web version of this article.)*

concentration of the PFCE-particle loaded DCs was estimated to be 40 pmol/cell by using ^{19}F MRI, and the detectability limit was 1000 cells μl^{-1} and 250 cells μl^{-1} for 40 min and 3 h acquisition, respectively. Moreover, OVA-PFC particles were proved to successfully activate antigen-specific $CD8^{+}$ T cells and inducing their proliferation *in vitro*. However, this interesting theranostic study lacks important *in vivo* experiments.

4.4. FLAMEs

An attractive mechanism was developed by Matsushita et al. [73] in order to address the instability of PFC nanoemulsions in organic solvents, which remarkably limit their application. They formulated PFCE-encapsulated silica nanoparticles, also known as FLAMEs (Fluorine accumulated silica nanoparticles for MRI contrast enhancement). These

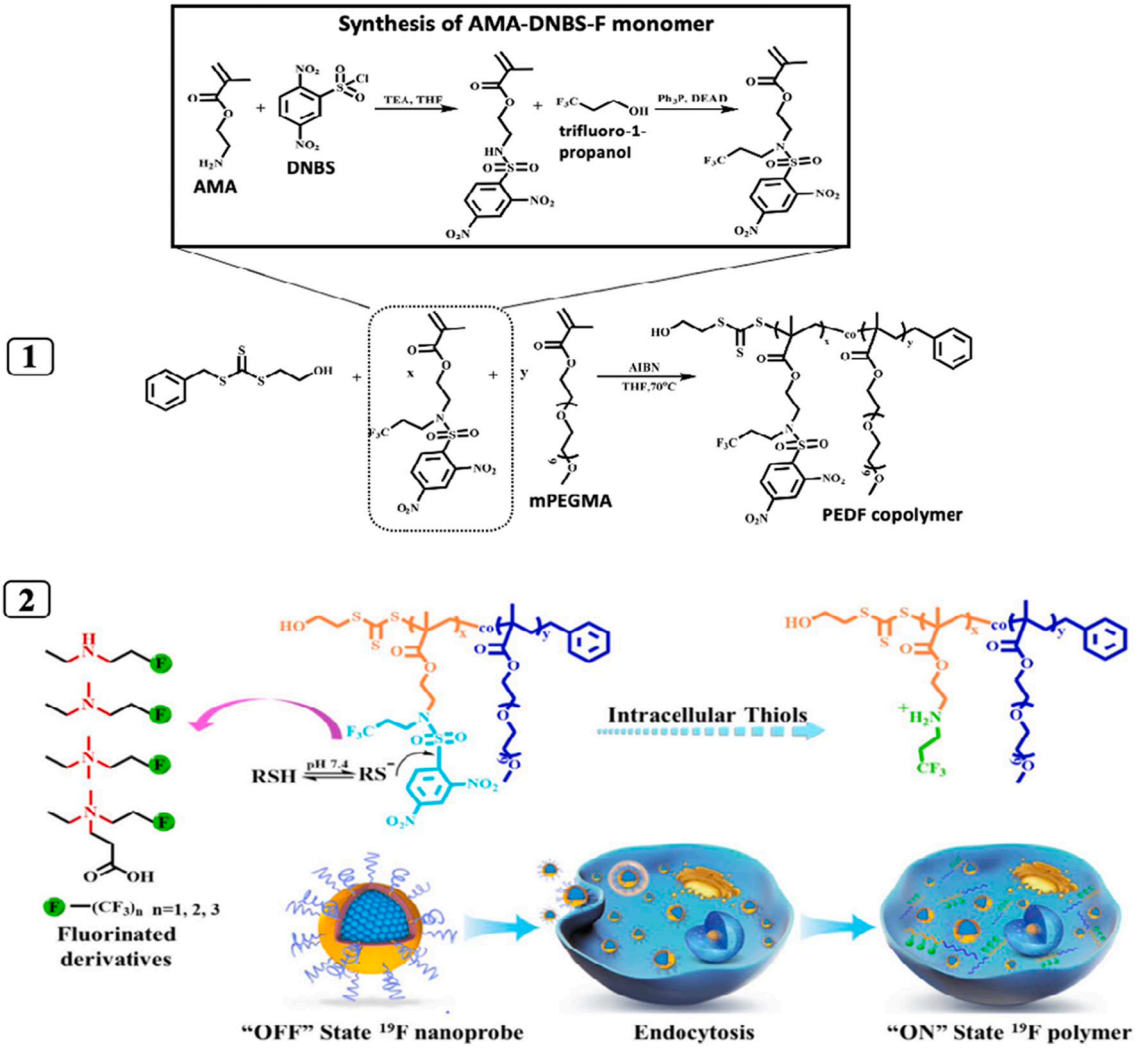

Fig. 8. (1) Synthesis of the p(mPEGMA)-*co*-poly(AMA-DNBS-F) (PEDF) copolymer and of the AMA-DNBS-F monomer. (2) ^{19}F nanoprobe design for specific imaging of bio-thiols. Fluorinated segments are tightly entrapped into the hydrophobic core, resulting in restricted chain mobility and ultrashort T_2 ("OFF" State). In the presence of intracellular sulfhydryl, the (2,4-dinitrobenzenesulfonyl)-groups are cut out from the polymer with a nucleophilic substitution reaction and the secondary amino group is protonated. Both polymer modifications cause disturbance of the hydrophilic/ hydrophobic balance, thus provoking nanoprobe disassembly and consequent enhancement of the ^{19}F-MRI signal ("ON" State), because of the increasing fluorinated chains mobility. Reprinted with permission from ref. [80]. *Copyright © 2018, American Chemical society*

NPs consisted of PFCE-liquid cores, which allow PFCE to reach a long T_2 due to its high mobility, and a thick silica shell. The hydrodynamic diameter of FLAMEs was about 131 nm and they showed a single peak by ^{19}F NMR spectroscopy. For ^{19}F-MRI sensitivity evaluation, ampicillin-modified FLAMEs (FLAME-Amp) were prepared and compared to smaller molecule-based probes. Silica NPs entrapped a high amount of ^{19}F atoms, therefore enhancing MRI sensitivity. Only the nanomolar amounts of the target protein were required for ^{19}F NMR detection. In contrast, micromolar range was needed for small-molecule probes, since they covalently bound to the proteins, limiting their mobility, which provoked T_2 shortening and a subsequent MRI signal reduction. Accordingly, using silica-envelope nanoparticles for biomedical applications has many advantages such as higher hydrophilicity and stability in aqueous and organic solutions and editable surfaces for nanoparticle functionalization. From *in vivo* experiments [73] it emerged that the PEGylated silica-nanoparticles mainly accumulate in the liver ($C_{PFCE} = 113$ nmol g^{-1}) and some ^{19}F signals was also detected at the tumor site ($C_{PFCE} = 28.8$ nmol g^{-1}), but no signals were detected from spleen, lungs, brain, kidneys and heart. On the other hand, the ^{19}F signals of intravenously injected non-pegylated silica nanoparticles were identified only in the liver, since they are immediately entrapped by the RES.

The same group moved forward with the same nanotechnology by developing multifunctional mesoporous silica nanoparticles (MSNs) as theranostic probes [74] (Fig. 6). Mesoporous FLAMEs (mFLAMEs) display an extraordinarily large surface area, tunable pore sizes (1.5–10 nm) and they may easily undergo several surface modifications for active targeting. They are composed of a PFCE-liquid core and a mesoporous (pore width of 6.7 nm) Cy5 dye-silica shell. ^{19}F-MRI and fluorescence are usually employed simultaneously in order to synergize the advantages of each modality (deep penetration and high sensitivity, respectively [75]). Once confirmed that the ^{19}F relaxometry was not altered in the formulation ($T_{2\ mFLAME} = 0.211$ s and $T_{2\ PFCE\ nanoemulsion} = 0.242$ s), folate (FA)-functionalized mFLAMEs were synthetized for tumor targeting. FA-mFLAMEs have been found to be stable in water solution up to 7 days after preparation, biocompatible, and to achive a 6.5-time increased cellular uptake compared to their controls. mFLAMEs were loaded with Doxorubicin to prove their theranostic success and their drug release seemed to be enhanced in acidic environments [74].

Considering the above-mentioned favourable features of mesopouros

silica nanoparticles, Chen et al. [76] designed pH-responsive nanoprobes for cancer diagnosis, based on the hexafluorobenzene-encapsulation into MSNs capped with gold nanoparticles (Au NPs). They are covalentely bound *via* hydrazone linkers, aiming to avoid an early release of the contrast agents from the nanopores. Specifically, at neutral pH the synthetized system did not allow nanoparticles to release the hexafluorobenzene, and consequently the ^{19}F signal was turned off. In an acidic environment, such as the cancer cell intracellular compartment, the hydrozone linkers were cleaved, the contrast agent released from the MSNs gates, and the MRI signal was turned on due to the shorter T_1.

4.5. Nanocrystals

Aside from PFC usage, inorganic nanocrystals are another interesting category of nanoprobes for ^{19}F MR imaging, but still with several correlated limitations. In this regard, Ashur et al. [77] formulated water-soluble calcium fluorinated nanocrystals with the intention to produce smaller versatile nanoparticles (about 10 nm) with improved delivery and clearance properties. However, the major drawback of these nanoprobes was the limited mobility of fluorine atoms which provoke a short T_2 and a long T_1 making them less effective for ^{19}F-MRI compared to other probes (Table 3).

5. Fluoropolymers or fluorolipids-based nanoprobes

Fluorinated contrast agents based on nano-emulsions to entrap a liquid perfluorocarbon have been largely studied and employed over the years. However, PFC emulsions suffer from important drawbacks as imaging contrast agents, such as their lipophilicity and accumulation in organs (liver, spleen, lungs) for long time. Furthermore, emulsion droplets are heterogenous and with a high probability to disintegrate inside the body. Moreover, such formulations have shown a prolonged T_1 relaxation time (more than 1000 ms at 1.5 T) [78].

5.1. Micelles

In order to address those relevant drawbacks, Du et al. [78] synthesized hyperbranched polymers carrying a high number of fluorine atoms. The synthetized hyperbranched fluoropolymers self-assembled into micelles in aqueous solution (Fig. 7), whose size ranged between 20 and 25 nm. They exhibited a narrow single peak in their ^{19}F NMR spectra, assuming a high mobility of the fluorinated group. T_1 and T_2 value emerged to be fairly short (about 500 ms and 64 ms, respectively) compared to PFCE or other small molecules. However, they showed a great ^{19}F imaging capability, with an adequate SNR (in the range of 32–11), and a linear correlation between SNR and fluorine concentration.

Later on, many other studies were conducted on ^{19}F copolymer synthesis intended for ^{19}F-MRI. Indeed, Jiang et al. [39] synthesized a bispherical perfluorocarbon molecule, termed ^{19}FIT ([19]F imaging tracer), using the modular symmetry strategy which implies both repetitive deprotection and condensation cycles. The several fluorinated groups in the hyperbranched probes may have intensified MRI signals and performance, and at a critical concentration of 7 mM they formed micelles, when dissolved in PBS. The 27 equivalent fluorine atoms gave rise to a single ^{19}F peak with a significantly short T_1. From the MRI phantom analysis, it emerged that the detection limit was 126 mM and from an *in vivo* study the half-life was estimated to be about 0.5 day without any evidence of organ retention or degradation. However, ^{19}FIT application to drug or cell tracking has displayed some key issues, such as sensitivity and the mechanism to link drugs to the probe. Indeed, if an intermolecular bond is used, it might dissociate from the target. But if a covalent bond is employed, it might compromise cells or drug bioactivity. However, the authors proposed to exploit a prodrugs mechanism in order to address these challenging issues.

Branched polymers are an interesting approach in which ^{19}F atoms preserve a high molecular mobility, which is crucial for proving a long enough T_2, which consequently generates a strong [19]F signal and adequate MRI image quality.

In general, micelles are conventional nanocarriers formed by a self-assembly method of amphiphilic molecules. They consist of a hydrophobic core and hydrophilic shell that may be modified for prolonging their circulation lifetime. Indeed, one of the most significant micelle shortcomings is their lack of stability in biological fluids [79].

Huang et al. [80] recently designed ^{19}F nanoprobe for specific imaging of bio-thiols for pathological assessment. Firstly, the copolymer was synthesized by using the previous prepared monomer by RAFT (reversible addition-fragmentation chain transfer) polymerization, which is a controlled radical technique for the synthesis of block and hyperbranched copolymers. Then, the nanoprobe was formulated by the nanoprecipitation technique. The nanoprobe hydrophobic core consisted of trifluoromethyl-containing segments whose assembling resulted in restricted chain mobility and ultrashort T_2 ("off" state). In the case of intracellular bio-thiols (*e.g.* cysteine, homocysteine and glutathione), nanoprobes disassembled due to the secondary amino groups' protonation, hence, the polymer regained its original flexibility, enhancing the ^{19}F-MRI signal ("On" state) (Fig. 8). The system, upon thiol treatment, showed a great T_2 value at a 7.0 T and a signal to noise ratio which increased 15-times, when compared to the starting time point. The developed nanosystem was injected into tumor-bearing mice at a fluorine dose of 378 μmol/kg and imaged at several time point. The signal intensity was particularly low after 2 h post injection and it became significantly stronger after 4 and 8 h. This indicates that the injected nanoprobes might be able to react with glutathione and cysteine in a tumor reducing microenvironment.

Accordingly, the emerging class of fluorinated polymers are considered as a potentially new generation of ^{19}F-MRI contrast agents. They have a number of advantageous features, such as a high fluorine content, low cytotoxicity, small particle size, and a versatile molecular structure which may undergo modifications for polymer functionalization. However, due to their hydrophobicity, in aqueous solutions, fluorinated segments may aggregate, therefore, reducing their mobility which provokes T_2 shortening and poor-related MRI signals. In other words, the transverse relaxation time (T_2) strongly depends on the dipolar coupling strength between ^{19}F atoms and other fluorine molecules around them, which influences their arrangement and hence mobility. However, a short T_1 for minimum scan time and a long T_2 are required for successful *in vivo* imaging acquisition. Moreover, as the polymerization procedure mostly occurs *via* ATRP (atom transfer polymerization) or the RAFT technique, it is necessary to consider the potential close proximity between fluorine atoms and the polymerizable moiety, since they may strongly decrease moiety electron density and its reactivity for further polymerization.

5.2. Polymeric NPs

An interesting mechanism to prevent fluorine-fluorine interactions was later developed by Wang et al. [81] They synthesized a pH-responsive and ^{19}F-containing star polymer, which may directly form nanoparticles in PBS. Nanoparticle core consisted of 2-(dimethylamino) ethyl methacrylate (DMAEMA) a pH-responsive material, fluorinated TFEA (2,2,2-trifluoroethyl acrylate) monomers and EGDMA (ethylene glycol dimethacrylate) which inhibited TFEA monomers aggregation by fluorinated segments hydration. Conversely, the hydrophilic shell encompassed PPEGMA brush polymer chains. According to cryo-TEM analysis, nanoparticles had a spherical shape with a diameter between 20 and 25 nm at pH 6. Moreover, nanoparticles displayed a strong major peak at −72.7 ppm and a long T_2 value under acidic conditions. However, different pHs seemed to influence nanoparticle size, the organization of the polymer chains and T_2 relaxation time. Indeed, at a pH above the pK_a, irregular particles were observed, the T_2 value

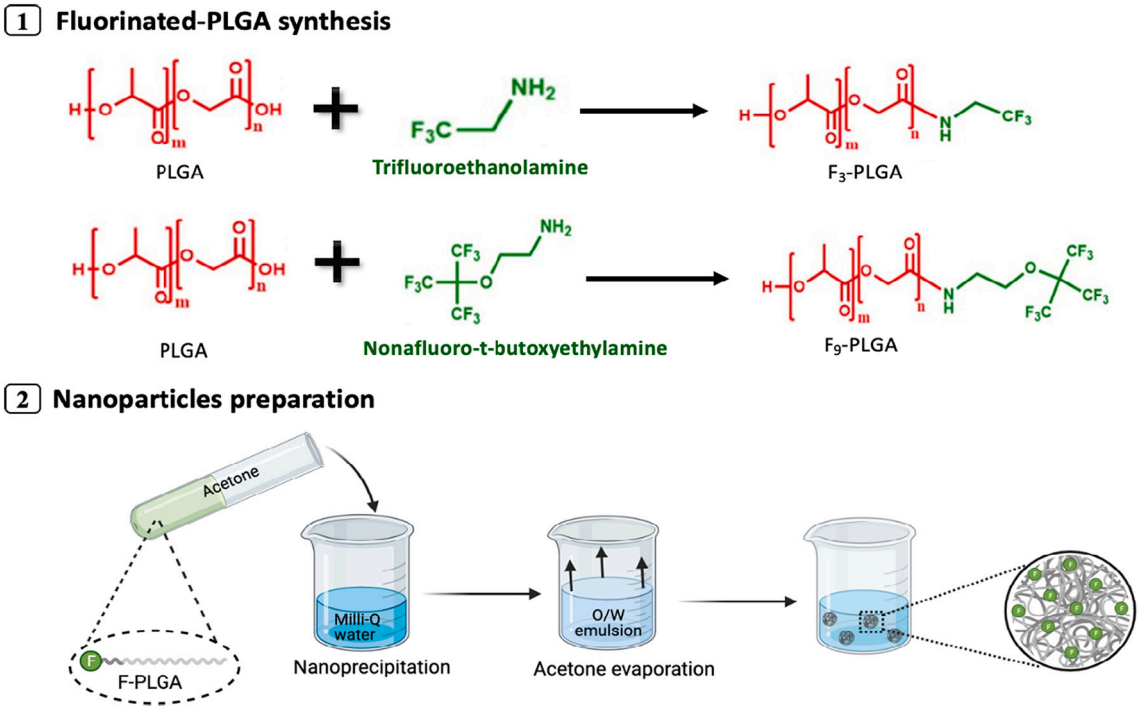

Fig. 9. Synthetic scheme of Fluorinated-PLGA copolymers (1) and F-PLGA nanoparticles preparation by nanoprecipitation techniques (2).

significantly decreased, and phantom detection was not possible due to the lack of signals. After approving the feasibility of this approach, the same group continued optimizing the RAFT polymerization technique for the synthesis of further pH-responsive polymers to selectively image tumor tissues [82], and for the multimodal polymer formulation nanoparticles in order to merge the high resolution of ^{19}F-MRI and the fluorescence imaging sensitivity [83]. However, only the multimodal nanoprobe has been tested *in vivo*, showing a localization of the non-targeted system mainly in the bladder and in the kidney, indicating that the system is small enough to be excreted *via* the kidney [83]. Indeed, they also evaluated the correlation between the nanoparticles' size and biodistribution/pharmacokinetics. Nanoparticles having a size about 7–8 nm showed a fast clearance in contrast to a prolonged circulation for NPs having a size that exceeds 11 nm. Nonetheless, when the system is functionalized with the folate targeting group, a strong ^{19}F signal was observed in the region of the tumor and liver in addition to the kidney and bladder. The accumulation of the system in other organs could be explained by the fact that folate receptor is also expressed by healthy tissue in liver and kidneys. The presence of the system in other organs were also confirmed by fluorescence analysis.

Besides previous controlled radical polymerization techniques, other methods have been used for fluorinated copolymers synthesis like the free-radical polymerization method.

For instance, this technique was employed by Bailey et al. [84] for the synthesis of polymeric nanoparticles for biomedical imaging using ^{19}F-MRI. Nanoparticles were formulated *via* a copolymerization technique between two different fluorinated monomers and N-vinyl formamide. Afterwards, surface amide groups were hydrolyzed to primary amines, hence, creating free reactive sites for potential functionalization in order to target specific pathological sites. The prepared nanoparticles were between 200 nm and 400 nm in diameter, and they showed a single resonance peak in ^{19}F NMR spectra. However, nanoparticles have not been studied by ^{19}F-MRI to define the minimal concentration for obtaining a sufficient signal for MR imaging neither *in vitro* nor *in vivo* preclinical studies.

Otherwise, Nurmi et al. [85] synthesized partially fluorinated polyelectrolytes as polymers for nanoparticle preparation and examined their applicability as an ^{19}F-MRI agent. Polyelectrolytes were either statistical (sequential distribution of the monomer relied on statistical rules) or block copolymers (different polymer chains linked together) of trifluoroethyl methacrylate (TFEMA) and 2-(dimethylamino)- ethyl methacrylate (DMAEMA). The statistical copolymers were directly dissolved in water, while the block ones were assembled into aqueous nanoparticles, composed of a kinetically frozen PTFEMA core and P(TFEMA-*co*-DMAEMA) corona. TFEMA, selected as the fluorine-containing monomer, was less hydrophobic than other fluorinated monomers. Hydrophobicity is an important parameter as it increases aggregation and reduces MRI signal intensity. pH variation impacts nanoparticle hydrodynamic diameter and ^{19}F NMR relaxations times and SNR. The ^{19}F NMR phantom analysis showed that it was possible to obtain high sensitivity images, if the ^{19}F nuclei had sufficient mobility. Nanoparticle imaging performance failed to meet expectations, but it may be improved by increasing the number of fluorine atoms and retaining the fluorine group mobility. The T_2 and T_1 values were suitable for *in vitro* and *in vivo* tests, which were not carried out.

A totally different approach for a formulation of fluorinated polymeric nanoparticles has been recently investigated by Neri et al. [86] They described a new nanotechnology platform called F-PLGA nanoparticles for multifunctional drug delivery. The synthesized F-PLGA copolymers were used to formulate PLGA nanoparticles by a nanoprecipitation method under surfactant-free conditions (Fig. 9). NPs showed a single ^{19}F NMR peak and suitable T_1 and T_2 values for ^{19}F-MRI applications. Fluorinated drugs were encapsulated in order to demonstrate nanoparticle efficiency for drug delivery. Compared to the unmodified PLGA nanoparticles, F-PLGA encapsulated an extended amount of drugs, even if the T_2 value of the loaded-F-PLGA nanoparticles decreased, suggesting a lower mobility of fluorine atoms after drug encapsulation. They also demonstrated *in vitro* the biocompatibility of nanoparticles and their efficacy in drug releasing studies. It seems evident that this field is still being broadly uninvestigated, therefore further studies are needed in order to translate these encouraging data into biological applications.

In general, fluoropolymer-based micelles and nanoparticles when compared to liquid perfluorocarbon-encapsulated nanoprobes, appear

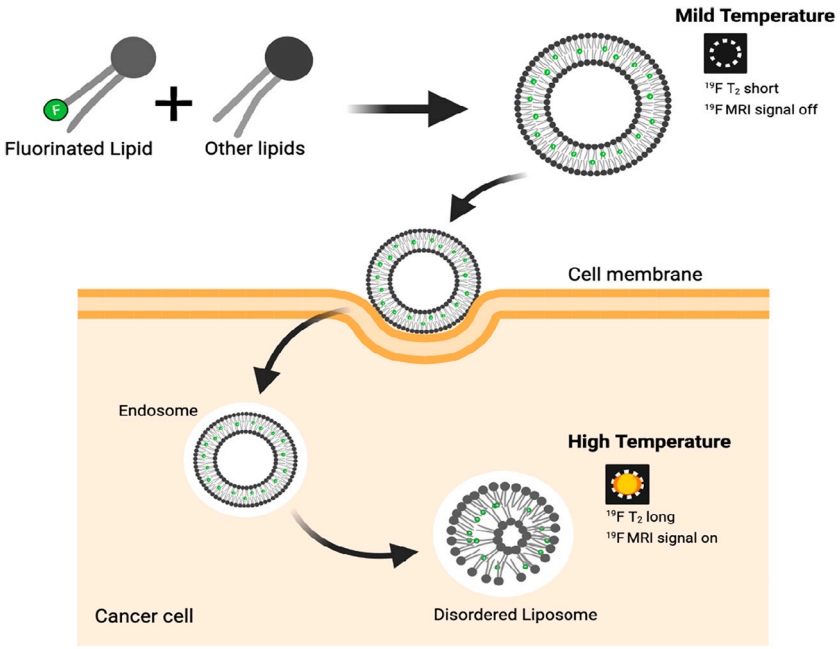

Fig. 10. Schematic representation of the use of fluorinated lipids employed for the formulation of temperature-sensitive liposomes. These liposomes are taken up by tumor cells *via* endocytosis and at elevated temperatures they transform into a disordered open state with an increase rotation of the fluorine group, which correspond to the ^{19}F NMR signal off-on switching.

to carry fewer fluorine atoms. The lower amount of fluorine atoms provokes a long acquisition time which may interfere with a successful *in vivo* analysis.

5.3. Dendrimers

Fluorinated dendrimers are another class of nanocarriers which have been intensively studied. Yet their formulation as MRI probes has never turned out to be practically applicable. Dendrimers are a class formed by hyperbranched repeated units with a greatly controlled structure; consisting of a central core, repeated units and shell functionalities.

In 2010, Owaga M. et al. [87] developed fluorinated dendrimer polymer nanoparticles by atom-transfer radical polymerization (ATRP) of fluorinated methacrylate monomers. Nanoparticles showed a spherical structure with an average hydrodynamic diameter in the range of 3–25 nm. Critical aspects of the study have emerged regarding T_1 and T_2 values, which were found to be too much shorter if compared to the common PFCs. Later on, the same group endeavoured to improve the formulation using a similar synthetic protocol. They managed to synthesize water soluble sphere-like structured nanoparticles loaded with a high fluorine load. The biocompatible NPs had to have two resonance peaks at −124 and − 138 ppm with a reasonable short T_1 value, which was beneficial for obtaining images with a fast repetition time, but still with a reduced T_2 value [88]. Basically, on the one hand, dendrimer-based nanoprobes may provide a high fluorine amount for an intense signal and often show a symmetric structure providing a single resonance peak, but on the other hand, their production is not as straightforward as expected [12].

Dendrimers are largely employed and studied as polymeric gene vectors as well, and fluorination of those nanocarriers has been shown to improve transfection efficacy and decrease cytotoxicity [89]. Therefore, they may be used as smart MRI theranostic probes, which ensure precise diagnosis and concomitant treatment of a particular disease [90].

5.4. Liposomes

In 2016, Xiao et al. [91] designed new liposome-like nanometric structures, also known as dendrimersomes. They were formulated by self-assembly of amphiphilic fluorinated dendrimers in water or buffer and displayed an unilamellar or multilamellar shape depending on the composition of the hydrophobic chains. Dendrimersomes can be considered as promising nanocarriers for ^{19}F-MRI studies, but further in-depth tests are needed to prove their potentiality.

Ren et al. [92] have recently proposed temperature-sensitive and non-encapsulated fluorinated liposomes. Fluorinated lipids were synthesized and mixed with other non-fluorinated lipids. Liposomes, obtained by the thin film hydration method followed by membrane extrusion, showed a hydrodynamic diameter of 185.1 nm and a zeta potential of −9.1 mV. At mild temperatures, the ^{19}F NMR signal is suppressed, due to the limited mobility of fluorine inside the liposome bilayer. A signal enhancement may be achieved at 39 °C (approximately lipid phase transition temperature), for the T_2 value increases when the well-organized liposomal structure is disassembled (Fig. 10). However, more *in vitro* and *in vivo* studies are needed to prove the potential efficacy of both studies.

5.5. Nanogels

Nanogels are another worth mentioning class of polymeric fluorinated agents. In general, nanogels can be considered as an ideal and versatile theranostic platform, since several formulation methods and a wide range of constituents are available for their preparation. Moreover, they are highly biocompatible, due to their extended water content, strong stability, and responsiveness to changes of stimuli like temperature, pH, or ionic concentrations. The controlled kinetic release is another interesting feature of this system; which is strongly dependent on the core crosslinking density and stimuli for which it is sensitive to [93].

Oishi et al. [94] proposed and designed a pH-activated ^{19}F-MRI nanogel probe. The system consists of a cross-linked polyamine (DEAMA: pH-sensitive element) gel core containing ^{19}F- bearing 2,2,2-trifluoroethyl methacrylate (TFEMA) and grafted PEG chains holding an acetal group at the α-end, which is needed as an active group for ligand attachment. At physiological pH, the nanogel core turned into a solid state because of the DEAMA amino group deprotonation, thus the TFEMA ^{19}F nuclei mobility was restricted causing a weak ^{19}F MR signal

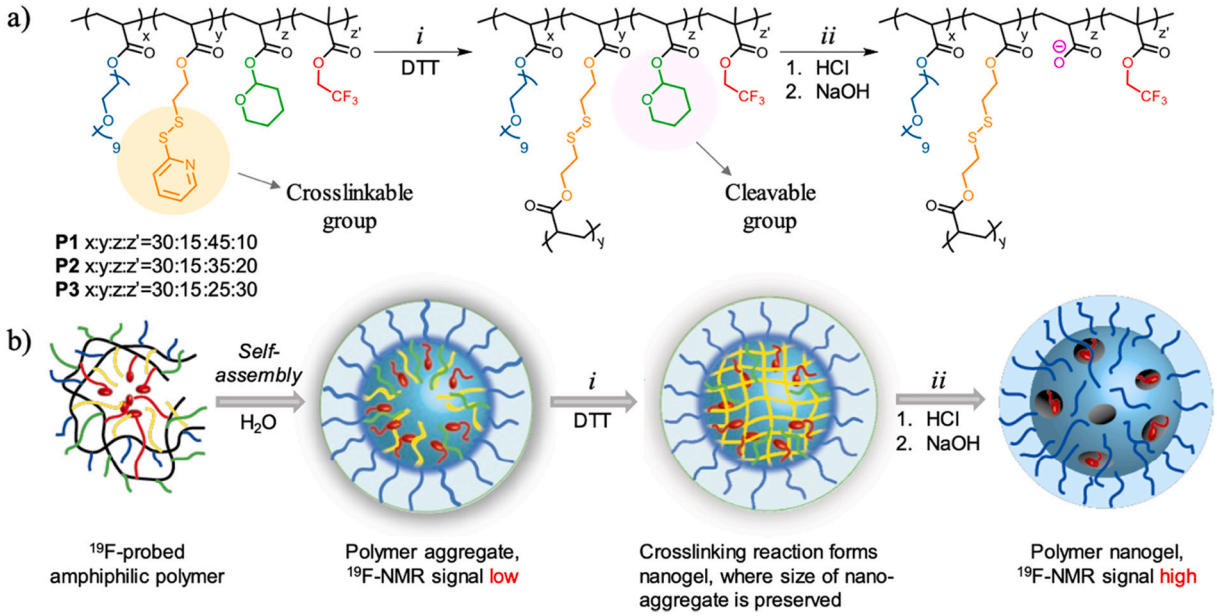

Fig. 11. (a) Polymer chemical structure and nanogel preparation. (*i*) Nanogel formation occurs *via* crosslinking of the pyridyldisulfide (PDS) groups in the presence of DTT. (*ii*) In acidic solution (HCl), the tetrahydropyranyl (THP) group is removed resulting in a negatively charged moiety formation with NaOH addition. (b) Schematic representation of fluorinated nanoprobe preparation and its decreased interior density resulting from the acid-catalyzed removal of the THP. Reprinted with permission from ref. [95]. *Copyright © 2019, American Chemical Society.*

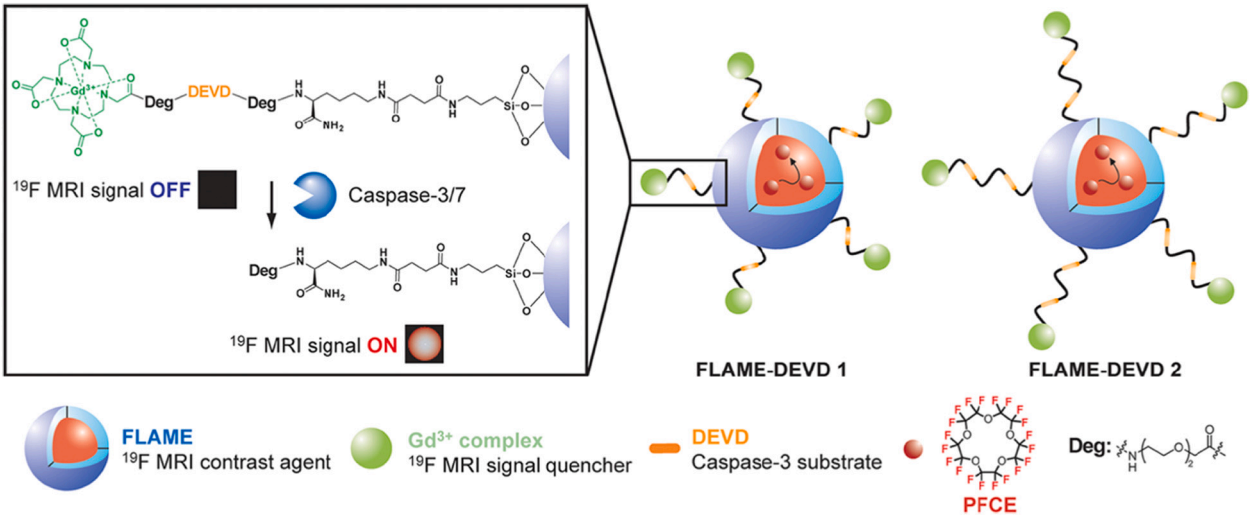

Fig. 12. Schematic illustration of FLAME-DEVD X (X = 1,2) for detecting apoptosis by caspase-3/7 activity. The ^{19}F nanoprobe On/Off switching mechanism is based on the paramagnetic relaxation enhancement effect of Gadolinium. DEVD corresponds to the caspase-3/7 substrate peptide sequence tandemly repeated X times. Reprinted with permission from ref. [106]. *Copyright © 2018, American Chemical Society.*

Table 2
Ongoing ^{19}F MRI clinical studies for cell labeling and tracking.

Clinical study identifier	Aim	^{19}F nanoprobe
NCT02035085	Track stromal vascular fraction (SVF) cells	CS-100 (PFPE-based nanoemulsion)
NCT02921373	Track peripheral blood mononuclear cells	CS-100 (PFPE-based nanoemulsion)
NCT02574377	Track myeloid and plasmacytoid blood dendritic cells	PFCE-PLGA nanoparticles

similar to the background one. Conversely, at a slightly acid tumor environment, an enhanced ^{19}F-MRI signal was reported as amines were protonated and PEGylated nanogels became hydrophilic and swollen. Interestingly, the highest ^{19}F-MR signal was achieved when the formulation contained 10 mol% TFEMA, the lowest concentration used; and the signal intensity linearly decreased as TFEMA amount increased.

The ability of fluorine atoms mobility to influence both T_1 and T_2 values, in particular spin-spin relaxation time, was also exploited by Munkhbat et al. [95], who designed stimuli-responsive polymeric nanogels. They synthesized random copolymers that contained PDS (pyridyl-disulfide) cross-linkable, fluorinated, and cleavable groups by the RAFT polymerization technique. The amphiphilic polymers in PBS spontaneously formed micelles, after which nanogels were formulated by PDS crosslinking when DTT (dithiothreitol) was supplemented. In the presence of NaOH or HCL, the THP (tetrahydropyranyl) group hydrolyzed, causing a partial degradation of the hydrophobic interior which correlated to T_2 enhancement (Fig. 11). They remarkably noted that as

Table 3
Selected examples of ^{19}F-encapsulated nanoprobes for ^{19}F-MRI.

Technology	Formulation components	Advantages	Limits	Size
PFPE nanoemulsion [48]	Perfluoropolyethelene glycol, Pluronic, dialkylcarbocyanine dye	- High (2.2×10^{13}) fluorine content per cell - Labeling procedure did not interfere with the T cell homing to the pancreas - NPs were not cytotoxic and did not stimulate T cells *in vitro*	- PFPE has 2 resonance peaks. However, the minor peak is below MRI detectability in vivo - ex vivo labeling - Transfection agents were used	103 ± 4 (nm)
PFCE encapsulated Silica NPs [73]	Rhodamine B isothiocyanate, Distearoyl-sn-glycero-3-phosphocholine (DSPC), 2-Phenylaminopyrimidine (PAP), PFCE, tetraethyl orthosilicate (TEOS)	- High sensitivity - Surface modifiability - *In vitro* stability - Biological inertness - Highly sensitive ^{19}F-MRI	- FLAMEs detected by ^{19}F-MRI mainly in spleen and liver	131 ± 1 (nm)
PFH/PFCE liposomes [72]	1,2-dioleoyl-3-trimethylammonium-propane (DOTAP), 1,2-dioleoyl-sn- glycero-3-phosphoethanolamine (DOPE), 1,2-distearoyl-sn-glycero-3-phosphoethanolamine- N-[amino (polyethylene glycol)-2000] (DSPE-PEG), cholesterol, Cholesteryl BODIPY® FL C12, PFH, PFCE, ovalbumin	- Non-toxic nanosystem - High fluorine concentration per cell (40×10^{12} for PFCE and 10^{12} for PFH) and a shorter acquisition time - The nanosystem does not induce any changes in DC phenotype - Layer by layer principle allows the carrier to load an increased amount of the relevant proteins	- Cells loaded with PFCH are more difficult to detect	PFH liposomes: 1.21 ± 1.28 (μm) PFCE liposomes 1.42 ± 1.84 (μm)
PFCE emulsion [54]	Egg lecithin, rhodamine DHPE (dihexadecanoic phosphatidylethanolamine), PFCE	- Cells are labeled successfully *in vivo* - Acceptable acquisition time	- The required field strength is too strong for translational purposes	130 (nm)
PFOB-loaded PEG-PLGA nanocapsules [57]	PLGA-PEG copolymer, polyvinyl alcohol (PVA), Sodium cholate, PFOB	- PLGA ensures good stability of the system and mechanical strength - Versatility of chemical moieties for a further functionalization - PEG increases plasmatic half-life - 85% of PFOB encapsulation efficiency	- Difficult to yield a good PEG coverage. Due to capsule formulation PLGA is sensitive to interfacial phenomena - Nanoprecipitation technique does not fulfill the requirements for the nanocapsules production in terms of size, PDI and encapsulation efficiency	121 ± 2 (nm)
PFCE-mFLAMEs [74]	Cy5–3-Aminopropyltriethoxysilane (Cy5-APTES), *n*-cetylammonium bromide (CTAB), PFCE, tetraethyl orthosilicate (TEOS)	- The silica shell ensure solubility in water, chemical surface modifiability, biocompatibility, efficient drug loading, release capacities	- Long acquisition time	165 ± 8 (nm)

Table 4
Selected examples of Fluoropolymers or fluorolipids-based nanoprobes.

Fluorinated segment	Main components	Chemical process	Formulation type	Size (nm)	Biomedical Application
Trifluoroethyl methacrylate (TFEMA) [78]	4-chloromethyl styrene (CMS), lauryl acrylate (LA), 1,1,1-tris(4′- (2′′-bromoisobutyryloxy)phenyl) ethane (TBBPE), tert-butyl acrylate	ATR-SCVCP*	Micelle	20–25	n/a
3, 3, 3-trifluoro-1-propanol [80]	2, 4-dinitrobenzenesulfonyl chloride (DNBS), 2-amino-ethyl methacrylate hydrochloride (AMA), Methyl Polyethyleneglycol Methacrylate (mPEGMA)	RAFT polymerization	Micelle	33.5 ± 1.8	Intratumoral imaging of bio-thiols
2,2,2-trifluoroethyl methacrylate (TFEMA) [82]	2-(dimethylamino) ethyl methacrylate (DMAEMA), Poly (ethylene glycol)methyl ether methacrylate (PEGMA), bis (2-methacryloyl)oxyethyl disulfide (DSDMA)	RAFT polymerization	Polymeric nanoparticle	About 23	pH-responsive probe for tumor imaging
Trifluoroethanolamine/ Nonafluoro-t-butoxyethylamine [86]	PLGA	Amide-coupling reaction	Polymeric nanoaparticle	54 ± 6/ 58 ± 6	Theranostic probe
2,2,3,3-tetrafluoro- propyl methacrylate (TFPMA), 2,2,2-trifluoroethyl methacrylate (TFEMA) [87]	PAMAM dendrimer with hydroxy- terminated groups (PAMAM-OH), 2- bromopropionyl bromide (BPB)	ATRP	Dendrimer	3–25	n/a
1-Ethynyl-4-(trifluoromethyl) benzene [92]	MPPC (1- myristoyl-2-palmitoyl-sn- glycero-3phosphocholine, DPPC(1,2-dipalmitoyl-sn-glycero-3-), MPEG-2000-DSPE (N-(Carbonyl-methoxypolyethyleneglycol 2000)-1,2-distearoyl-sn-glycero-3- phosphoethanolamine, sodium salt), lyso-PC(1-stearoyl-2-hydroxy-sn- glycero-3-phosphocholine), 4-Bromo-1,8-naphtalic anhydride	Covalent conjugation	Liposome	185.1	Temperature-sensitive nanoprobe
TFEMA (2,2,2-trifluoro ethyl methacrylate)/ 3,5- bis(trifluoromethyl) benzoic acid/ nonafluoro-tert-butyl alcohol [95]	PEGA (Polyethylene glycol monomethyl ether acrylate), PDSA (Pyridyl disulfide ethyl acrylate), THPA (2-tetrahydropyranyl acrylate), CHA (Cyclohexyl acrylate)	RAFT polymerization	Nanogel	8, 9, 9, 13, 52, 7, 12 **	Theranostic pH-sensitive nanoprobe

* Atom transfer radical self-condensing vinyl (co)polymerization.
** Size distribution of nanogels prepared with different synthetized polymer (P1, P2, P3, PC, P4, P5, and P6, respectively).

the T_2 value steadily increased, changing from polymer nanogels to acid-degraded nanogels, the T_1 preserved its value. The feasibility of fluorinated nanogels as nanoprobes for ^{19}F imaging was shown by *in vivo* tests in mouse models with induced inflammation [95]. Polymeric nanogel at ~650 mM fluorine concentration was intravenously injected, and mice were imaged by ^{1}H and ^{19}F MRI. Two hours after administration, a

considerable amount of ^{19}F signal was found in heart and carotid arteries, suggesting a long blood circulating time. The ^{19}F signal also remained strong enough after 72 h, mainly accumulating in the inflamed area. By the way, clearance and biodistribution studies are needed to evaluate the proper efficacy of the system, which may be a promising and customizable theranostic and multimodal imaging probe.

Both described nanogels were formulated by the cross-linking method of polymers, but self-assembly is another efficient method for the preparation of nanogels as described by Kolouchova et al. [96] In this study, nanogels consisted of an amphiphilic copolymer that contained hydrophilic biocompatible and fluorinated thermo-responsive blocks, which non-covalently interacted above a certain temperature. The system was biodegradable and checked to hold a high magnetically equivalent ^{19}F atom content. Moreover, T_1 relaxation times did not depend on temperature changes, therefore nanoprecipitation slightly influenced ^{19}F relaxation properties, meaning that fluorine mobility was not limited. By contrast, T_2 values were impaired by temperature changes due to the solvation of fluorine atoms in nanogels. The nanosystem was demonstrated to be biocompatible *in vitro* and to does not interact with red blood cells. However, thermoresponsive feature has not yet been demonstrated in mouse models.

Self-assembled nanomaterials have always aroused the interest of scientists in nanotechnology, because of their simplicity, spontaneity, scalability, and inexpensiveness. Those polymer systems are based on non-covalent interactions, such as hydrophobic or ion-ion bonds. According to the type of bonds and molecules, different nanocarriers may be developed by self-assembly in addition to the above-mentioned nanogels, such as polymer nanoparticles and micelles.

For instance, Babuka et al. [97] developed cross-linked nanogels based on a thermo-responsive copolymer, which exhibited a single resonance peak, and a gradual decrease in ^{19}F signal as temperature increased. However, alike the previous work, the ^{19}F NMR study revealed that T_1 and T_2 values were not strongly affected by temperature variations, hence, making it a promising ^{19}F-MRI tracer. However, the formulated nanoprobes have been assessed neither *in vitro* nor *in vivo* tests yet.

As previously analyzed, a plethora of fluorinated polymers have been designed and employed for the formulation of ^{19}F-MRI nanoparticles.

5.6. Nanoribbons

Fluorinated peptides have been synthesized and exploited as well. Amphiphilic peptides revealed to be biocompatible and highly functional for imaging purposes. In this regard, Preslar et al. [98] designed fluorinated amphiphilic peptides, which, in buffered, self-assemble into nanoribbons. Their width strongly depends on Ca^{2+} concentrations, hence, modifying fluorine signal intensity. In particular, as the nanoribbons became wider, the ^{19}F NMR signals decreased as a result of T_2 shortening. Interestingly, the Ca^{2+}-dependent on/off switching of nanoribbons did not completely imply disruption of assembly.

6. Tunable paramagnetic-^{19}F dual-nanoprobes

So far, perfluorocarbon nanoparticles and fluorinated biomaterials are the most commonly used probes, since they carry a high number of ^{19}F nuclei per molecule, which enhances the contrast-to-noise ratio. However, adding ^{19}F nuclei to a molecule for better MRI performance implies some limitations, such as maintaining an adequate hydrophilicity for *in vivo* applications and placing them in such a way that they prove to be all magnetically equivalent.

Using ^{19}F nuclei for MRI acquisition has several advantages, such as its absence in biological tissues, which enables unambiguous quantitative cell tracking [3]. However, its clinical translation may be challenging, because of the ^{19}F atom long longitudinal time (usually between 0.5 and 3 s) and low sensitivity; the probe concentration required for a sufficient signal to noise ratio is between 10 and 50 mM. In comparison, Gd-contrast agents require a lower concentration, namely 0.1 μM [99].

In order to address the sensitivity issue of ^{19}F-MRI techniques, other types of nanoprobes have been designed and explored over the years, in addition to the ones previously discussed, aimed at improving relaxation properties of PFC molecules.

In this regard, the combination of a paramagnetic center (*e.g.* Mn^{2+}, Fe^{3+}, Gd^{3+}), such as a metal ion or complex, with a ^{19}F nanoprobe, reduces ^{19}F T_1 values for a rapid image acquisition and increases the signal-to-noise ratio per unit time [100,101]. However, this approach may also provoke a T_2 reduction and line broadening of resonance signals. Notably, ^{19}F-lanthanide MRI nanoprobes, in which the fluorinated group is properly placed far from the paramagnetic center, have shown improved MRI sensitivity. This class of compounds should be thoughtfully designed, if ^{19}F-paramagnetic metals distances are too long, the sensitivity enhancement is almost negligible. On the contrary, if the paramagnetic center is too close to the ^{19}F atoms, the T_2 value decreases causing severe line broadening and signal intensity reduction [100–102].

Neubauer et al. [102] demonstrated the relaxation enhancement by attaching Gd^{3+} to the outer surface of PFCE nanoemulsion droplets. They formulated a pioneering PFCE nanoemulsion, using a comixture of lipophilic gadolinium-(Gd-DTPA-BOA), lecithin and dipalmitoyl-phosphatidylethanolamine as a surfactant. Gd^{3+}-ions were incorporated into the lipid monolayer that covered the PFCE emulsion and supposedly less far away than 15 Å from the PFCE core. The gadolinium proximity led to a four-fold increase in PFCE R_1 value at 1.5 T along with an increase in imaging sensitivity. Additionally, when the distance between the gadolinium complex and the NP surface increased, the T1 value was significantly affected.

A similar Gd^{3+}-based ^{19}F-MRI nanoprobe was reported by Kok et al. [103] to target the cell-internalizing$\alpha_v\beta_3$- integrin receptor that is highly expressed on human endothelial cells. Nanoparticles consisted of a PFCE core and amphiphilic gadolinium chelates (Gd^{3+} -DOTA-DSPE) emulsified in water using 1,2-Distearoyl-*sn*-glycero-3-phosphocholine (DSPC), cholesterol, and a mixture of PEG_{2A000}-DSPE and Mal-PEG_{2000}-DSPE. Emulsion droplets revealed an average size of 170 nm, a great stability up to 80 days after formulation, and a spherical shape shown by cryo-TEM images. The additional functionalization of the emulsion with a cyclic RGD-peptide ligand revealed an enhanced uptake by endothelial cells. The presence of Gadolinium in the formulation improved PFCE longitudinal and transverse relaxation times. Moreover, *in vitro* study of the HUVEC cell line showed that the uptake of the nanoemulsion did not affect the longitudinal relaxion time (T_1), whereas the T_2 value decreased when the concentration of the nanoemulsion wasincreased. Indeed, the lower intracellular pH caused an enhanced gadolinium release, thus altering the observed relaxation properties of the ^{19}F atoms.

Paramagnetic fluorinated nanoparticles have also been investigated for the concomitant and synergic acquisition of both ^{1}H and ^{19}F MR images. Morawski et al. [104] formulated biotinylated nanoparticles for a quantitative assessment by ^{19}F MRS in the targeted area. Simultaneous ^{1}H-MRI analysis, which colocalized with the ^{19}F signals, provided unequivocal anatomical information. The NPs were composed of 20% (*v*/v) of fluorinated core (PFCE or PFOB) emulsified in water with lecithin, cholesterol, and biotinylated dipalmitoyl-phosphatidylethanolamine, and 30 mol% of lipophilic gadolinium chelate, which strongly enhanced local R_1 relaxation rates. Monoclonal antibody ligands were included in the formulation to specifically bind to fibrin clots, as fibrin deposits in the vascular endothelium are indicative of a pathological condition. Nanodroplets' diameter was around 200–300 nm, and found to carry a large gadolinium and perfluorocarbons payload, thus reaching a high signal to noise ratio at adequate concentrations.

In an interesting study by Nakamura et al. [105], the interaction between paramagnetic metals and fluorinated MRI probes was exploited to image a reducing environment. In this case, the surface of FLAMEs was modified by Gd^{3+}-DTPA (diethylenetriamine-pentaacetate)

complexes, attached *via* bisulfide linkers. In a reducing environment, the disulfide group is reduced, and the Gd^{3+} complexes cleaved and released from the FLAME-SS-Gd^{3+} surface, breaking down the Gd^{3+} PRE (paramagnetic relaxation enhancement) effect on fluorine compounds. As a result, the PFCE T_2 value increased, and the ^{19}F-MRI signals were enhanced. However, the ^{19}F-MRI signals were highly faded without reducing agents due to the PRE effect efficiency [105].

In 2018, the same group made progress in this nanotechnology by designing the PFCE-encapsulated FLAMEs with an off/on ^{19}F-MRI switch for caspase-3/7 activity detection *in vivo* [106]. The surface-carboxylated nanoprobes were then decorated with the previously synthesized Gd^{3+} complex-conjugated DEVD2 peptides (Fig. 12). In the presence of caspase-3/7 activity because of apoptosis, the substrate peptide sequences were cleaved, thus allowing the ^{19}F-MRI signals to switch-on as a consequence of the Gd^{3+} complexes removal from the nanoparticles surface.

The potential of using FLAMEs and FLAME-DEVD2 was evaluated in C57BL/6Jjcl mice. As expected, FLAMEs injected in bloodstream are recognized by phagocytic cells, such as Kupffer cells and splenic macrophages, thus the ^{19}F signals were observed mainly in the liver and spleen. However, when FLAME-DEVD2 were injected, ^{19}F signals were detected in the liver, due to hydrolysis by liver proteases. After induction of apoptosis in macrophages in the liver, the signal to noise ratio from FLAME-DEVD2 turned out to be clearly enhanced by caspase-3/7 activity. In order to verify the accumulation of the nanoprobes in the spleen tissue, fluorescence imaging was conducted, and it emerged that they highly localize in the spleen regardless of apoptosis induction.

The fluorine-rich dendrimer-based nanotechnology in combination with gadolinium chelates (DOTA) was also considered to obtain some improvements in relaxation properties [107]. Phantom MRI studies revealed that as the dendrimers hydrodynamic radius increased the longitudinal relaxation time shortened at 11.7 T. However, the lowest T_1 value reached by increasing the dendrimers size was still relatively long for rapid imaging. Adding the Gd^{3+} to the chelate near the fluorine atoms drastically reduced the T_1 value. The main drawback of the synthesized dendrimers with a p -trifluoromethylphenylalanine surface remained their cytotoxicity measured by MTT assay. Fortunately, the toxicity may be reduced by shielding the fluorine groups into the dendrimer core. Indeed, this can prevent interaction between fluorine groups and reduce the hydrophobicity. One of the optimized compound were then analyzed *in vivo* in healthy rats by coinjection of the dendrimer and Gd^{3+}-CA (ProHance) *via* tail vein [107].

As already seen, gadolinium has been largely investigated as a lanthanide in combination with ^{19}F nanoprobes. However, some studies revealed that gadolinium is less effective than other metal ions.

In this regard, Kislukhin et al. [108] developed a series of paramagnetic fluorinated nanoemulsions using PFPE-base β-diketones (FDKs) as a metal chelator. Nanoprobes were formed by the addition of the FDKs to the aqueous phase of the pre-made PFPE nanoemulsion. This was followed by the supplementation of either $FeCl_3$ or $GdCl_3$ for the direct metalation of FDK nanoemulsions, enabled by the use of Pluronic as a surfactant which is permeable to ions. ^{19}F relaxometry of nanoemulsions was assessed in the presence of Fe^{3+} and Gd^{3+}, revealing that Fe^{3+} is more effective than Gd^{3+} as an R_1 agent. Indeed, Gd^{3+} showed a two-times lower R_1 and a severe ^{19}F NMR resonance line broadening than Fe^{3+} at clinical field strength. A crucial advantage of using β-diketones chelators (pAn-FDK) was their stability and capacity to irreversibly carry the metal ions even at the intracellular milieu, but it was less efficient when macrocyclic chelates were employed. Moreover, FETRIS (ferric *tris*-diketonate) was used to label *ex vivo* rodent glioma cells, rendering these cells biocompatible and readily taken up, however ^{19}F R_1 decreased by about 25% after labeling. Unlike the above-described studies, in the last example, the paramagnetic metal ion is incorporated into the fluorous core in order to decrease its distance from the ^{19}F atoms.

Such outstanding Fe^{3+} performance in their system was also demonstrated by Peng et al. [109]. They predominately focused on the design of new chelators and fluorine agents in order to optimize the number of fluorines which contributed to the generation of ^{19}F NMR signals. They prepared a fluorinated contrast agent consisting of 27 symmetric fluorine atoms and a diketone chelator already used [108]. In this study, the chelator was optimized by covalently linking the fluorinated moiety also used as a contrast agent. PFPE-based chelator was then emulsified to formulate different nanoemulsions, which were non-toxic on several cell lines. Despite the high number of fluorine atoms, the formulation generated a single resonance peak, as a result of its symmetry. Furthermore, both the Fe^{3+} paramagnetic effect and the maximization of the effective fluorine enhanced the ^{19}F-MRI sensitivity, which revealed to be sufficient for tracking cells in mice.

7. Conclusion and outlook

Despite the many advantages offered by ^{19}F-MRI techniques, such as the absence of the fluorine-19 atoms in biological tissues which enables cell tracking and quantitative analyses, many technical fluorinated compounds-related problems have emerged. Indeed, ^{19}F- probes designed thus far show long T_1 and short T_2 relaxation times. Furthermore, it is pretty arduous to obtain optimal ^{19}F MR images in case compounds with a too short T_2 relaxation time are used [110].

In order to improve MRI performance many efforts have been made to date. However, ^{19}F nanoprobes with excellent spectral properties, relaxation time, and signal sensitivity simultaneously, are still needed. Indeed, the success for an *in vivo* ^{19}F MR imaging assessment strongly depends on the MR properties of the ^{19}F probe, such as relaxation times and NMR spectrum (single or multiple peaks), which both influence the sensitivity of the ^{19}F-MRI techniques. Multiple peaks in the ^{19}F NMR spectrum are an adverse feature in terms of SNR and imaging quality, since they do not contribute to the same spectral peak [111].

Fluorinated biomaterial-based nanoprobes (Table 4) are one of the most promising classes of nanoprobes characterized by tailorable properties which enable them to be ideal for many biomedical applications, such as theranostic purposes or functional imaging in response to specific changes in physiological stimuli (pH, temperature, or ion concentrations) changes. Moreover, they hold a high number of fluorine atoms causing a high ^{19}F-MRI signal, and a low cytotoxicity.

Perfluorocarbons, because of their formulation into nanoparticles, have been proven to be biocompatible and clinically tested. However, new fluorinated contrast agents need to be synthesized to overcome their drawbacks such as long retention times and lack of symmetry or fluorine content. Their combination with a paramagnetic center appears to greatly increase ^{19}F nanoprobes efficiency. Indeed, paramagnetic fluorine probes are an interesting approach for increasing fluorine sensitivity, as a result of the R_1 reduction and chemical shift spectral window enhancement.

The capability of these nanoprobes to increase MRI sensitivity is contingent upon the magnetic field strength; in other words, they may be better detected with ^{19}F-MRI at low and medium strength (below 6 T) [99]. ^{19}F nanoemulsions without gadolinium, rather, need a magnetic field strength usually between 6.3 and 14 T [112].

Furthermore, biodegradable PLGA polymers have been extensively utilized for imaging and delivery purposes due to their ability to protect the encapsulated agents until delivery. Moreover, PLGA-nanoparticles have a high surface area, which is suitable for the attachment of targeting moieties or other materials, and the ability to modify the active agent biodistribution in a controlled manner. Another key element of these polymeric nanoparticles is their stability, because of the possibility to be frozen and lyophilized, thus making storage easier.

PLGA nanoparticles have been employed for both small fluorinated molecule encapsulation [32,57] and fluorine attachment [86] in order to synthesize the ^{19}F copolymer.

The several advantages derived from using PLGA-nanoparticles also as ^{19}F nanoprobes as well as their widespread use has driven some

research groups to investigate and optimize their scale up production [25]. Indeed, it has been shown that PFCE-PLGA nanoparticles when used for cell labelling do not affect cell viability, and cell function [113]. Nevertheless, current polymeric nanosystems suffer from some drawbacks such as the low accumulation at the target site and a rapid blood clearance. Indeed, the uptake of the intravenously injected perfluorocarbon-encapsulated PLGA NPs occurs primarily in spleen and liver [25,57]. Another crucial issue, which hamper the clinical translation, is their slow local clearance, causing a long biological retention. However, recently it has been demonstrated that the *in vivo* clearance rate strongly depends on the ultrastructure of the formulation [114]. The multi-core ultrastructure of the PFCs- PLGA nanoparticles makes the clearance profile a 15-fold faster than conventional lipid-based nanoemulsions and PLGA-based single core nanoprobes.

An appropriate probe for clinical translation should express some key features, such as (i) a high fluorine content to achieve sufficient signals for MRI analysis, (ii) an easy formulation and scale up procedure, (iii) high chemical and biological stability, with adequate half-life (iv) safety profiles *in vitro* and *in vivo*, (v) a simple ^{19}F NMR spectrum with a single and intense resonance peak, (vi) and short T_1 and long T_2 values.

Based on the above-mentioned ideal characteristics, only PLGA NPs and PFPE-based agents have been improved to express most of them and consequently implemented in clinical studies to label cells *ex vivo* (Table 2). Indeed, both of them lack selectivity when directly injected *in vivo*. Nevertheless, while PLGA NPs have an easily modifiable structure, PFPE nanoemulsions are difficult to further functionalize since the potential extra covalent bond might break the symmetry of the probe.

Fluorinated biomaterials may definitely fulfill features (i), (v) and (vi), but their chemical synthesis and formulation is quite complicated since they involve multiple steps, and it may turn out to hamper the scale up production. Further significant hurdles are their solubility in water and pharmacokinetic/pharmacodynamic properties including biodegradability and clearance of the nanoprobe.

A high number of studies have been carried out since the late 1990s, demonstrating that MR imaging of fluorine has always been a research topic and many pioneering probes have been designed in tandem with constant developments and the progress made in the study of nanomaterials. However, clinical applications of fluorinated nanoprobes for tumor imaging, pO_2 quantification and cell tracking are still minimal and the results obtained so far by ^{19}F-MRI are very preliminary but really promising [57,115,116]. Among the many applications of ^{19}F-MRI techniques, cell tracking is the area that has yielded the most successful results. Indeed, in 2014 the first patient was transplanted with therapeutic DCs labeled *ex vivo* with Cell Sense, a commercial PFC agent [28].

^{19}F-MRI is still in its infancy; however, from the-state-of-art a brighter and successful future can be foreseen in clinical applications, along with improvements in sensitivity and better understanding of cell labeling.

Declaration of Competing Interest

None.

Acknowledgements

This project has received funding from the European Union's Horizon 2020 research and innovation programme under the Marie Sklodowska Curie grant agreement No 859908 (NOVA-MRI) and by the VIDI personal grant (project number 723.012.110) L.J.C.

References

[1] P. Rinck, A short history of magnetic resonance imaging, Spectrosc. Eur. 20 (2008) 7–9.
[2] R. Bitar, et al., MR pulse sequences: what every radiologist wants to know but is afraid to ask, Radiographics 26 (2006) 513–537.
[3] M. Srinivas, A. Heerschap, E.T. Ahrens, C.G. Figdor, I.J. de Vries, 19F MRI for quantitative in vivo cell tracking 28, 2011, pp. 363–370.
[4] E.T. Ahrens, J.W.M. Bulte, Tracking immune cells in vivo using magnetic resonance imaging, Nat. Rev. Immunol. 13 (2013) 755–763.
[5] J.X. Yu, R.R. Hallac, S. Chiguru, R.P. Mason, New frontiers and developing applications in 19F NMR, Prog. Nucl. Magn. Reson. Spectrosc. 70 (2013) 25–49.
[6] J. Zhong, P.H. Mills, T.K. Hitchens, E.T. Ahrens, Accelerated fluorine-19 MRI cell tracking using compressed sensing, Magn. Reson. Med. 69 (2013) 1683–1690.
[7] G. Duan, X. Zhao, S.W. Anderson, X. Zhang, Boosting magnetic resonance imaging signal-to-noise ratio using magnetic metamaterials, Commun. Phys. 2 (2019) 1–8.
[8] J. Jokerst, T. Lobovkina, R. Zare, S. Gambhir, Nanoparticle PEGylation for imaging and therapy, Nanomedicine 6 (2011) 715–728.
[9] C. Giraudeau, et al., High sensitivity 19F MRI of a perfluorooctyl bromide emulsion: application to a dynamic biodistribution study and oxygen tension mapping in the mouse liver and spleen, NMR Biomed. 25 (2012) 654–660.
[10] J.S. Suk, Q. Xua, N. Kima, J. Hanesa, L.M. Ensigna, PEGylation as a strategy for improving nanoparticle-based drug and gene delivery, Adv. Drug Deliv. Rev. 25 (2016) 28–51.
[11] D. Jirak, A. Galisova, K. Kolouchova, D. Babuka, M. Hruby, Fluorine polymer probes for magnetic resonance imaging: quo vadis? Magn. Reson. Mater. Physics, Biol. Med. 32 (2019) 173–185.
[12] I. Tirotta, et al., 19F magnetic resonance imaging (MRI): from design of materials to clinical applications, Chem. Rev. 115 (2015) 1106–1129.
[13] J. Guenoun, et al., Cationic Gd-DTPA liposomes for highly efficient labeling of mesenchymal stem cells and cell tracking with MRI, Cell Transplant. 21 (2012) 191–205.
[14] C.L. Tseng, I.L. Shih, L. Stobinski, F.H. Lin, Gadolinium hexanedione nanoparticles for stem cell labeling and tracking via magnetic resonance imaging, Biomaterials 31 (2010) 5427–5435.
[15] C. Aspord, et al., Paramagnetic nanoparticles to track and quantify in vivo immune human therapeutic cells, Nanoscale 5 (2013) 11409–11415.
[16] P. Bouvain, S. Temme, U. Flögel, Hot spot 19F magnetic resonance imaging of inflammation, Wiley Interdiscip. Rev. Nanomed. Nanobiotechnol. 12 (2020) 1–21.
[17] H.S. Thomsen, Nephrogenic systemic fibrosis: a serious late adverse reaction to gadodiamide, Eur. Radiol. 16 (2006) 2619–2621.
[18] C. Yu, et al., In depth analysis of apoptosis induced by silica coated manganese oxide nanoparticles in vitro, J. Hazard. Mater. 283 (2015) 519–528.
[19] M. Bellusci, et al., Biodistribution and acute toxicity of a nanofluid containing manganese iron oxide nanoparticles produced by a mechanochemical process, Int. J. Nanomedicine 9 (2014) 1919–1929.
[20] A.K. Srivastava, et al., Advances in using MRI probes and sensors for in vivo cell tracking as applied to regenerative medicine, DMM Dis. Model. Mech. 8 (2015) 323–336.
[21] S.M. Cromer Berman, P. Walczak, J.W.M. Bulte, Tracking stem cells using magnetic nanoparticles, Wiley Interdiscip. Rev. Nanomed. Nanobiotechnol. 3 (2011) 343–355.
[22] S.M.C. Berman, et al., Cell Motility of Neural Stem Cells is Reduced after SPIO-Labeling, which is Mitigated after Exocytosis 69, 2013, pp. 255–262.
[23] E.J. Ribot, P.J. Foster, In vivo MRI discrimination between live and lysed iron-labelled cells using balanced steady state free precession, Eur. Radiol. 22 (2012) 2027–2034.
[24] E. Hequet, C. Henoumont, R.N. Muller, S. Laurent, Fluorinated MRI contrast agents and their versatile applications in the biomedical field, Future Med. Chem. 11 (2019) 1157–1175.
[25] E. Hoogendijk, et al., Continuous-flow production of Perfluorocarbon-loaded polymeric nanoparticles: from the bench to clinic, ACS Appl. Mater. Interfaces 12 (2020) 49335–49345.
[26] L. Zerrillo, et al., Novel fluorinated poly (lactic-co-glycolic acid) (PLGA) and polyethylene glycol (PEG) nanoparticles for monitoring and imaging in osteoarthritis, Pharmaceutics 13 (2021) 235.
[27] M. Wolters, et al., Clinical perspectives of hybrid proton-fluorine magnetic resonance imaging and spectroscopy, Investig. Radiol. 48 (2013) 341–350.
[28] A.V. Makela, et al., Cellular imaging with MRI, Top. Magn. Reson. Imaging 25 (2016) 177–186.
[29] E.T. Ahrens, B.M. Helfer, C.F. O'Hanlon, C. Schirda, Clinical cell therapy imaging using a perfluorocarbon tracer and fluorine-19 MRI, Magn. Reson. Med. 72 (2014) 1696–1701.
[30] M. Cametti, B. Crousse, P. Metrangolo, R. Milani, G. Resnati, The fluorous effect in biomolecular applications, Chem. Soc. Rev. 41 (2012) 31–42.
[31] D. O'hagan, Understanding organofluorine chemistry. An introduction to the C–F bond, Chem. Soc. Rev. 37 (2008) 308–319.
[32] M. Srinivas, et al., Customizable, multi-functional fluorocarbon nanoparticles for quantitative in vivo imaging using 19F MRI and optical imaging, Biomaterials 31 (2010) 7070–7077.
[33] I.J.M. De Vries, et al., Magnetic resonance tracking of dendritic cells in melanoma patients for monitoring of cellular therapy, Nat. Biotechnol. 23 (2005) 1407–1413.
[34] J.G. Riess, Perfluorocarbon-based oxygen delivery, Artif. Cells, Blood Substitutes, Biotechnol. 34 (2006) 567–580.
[35] L. Hu, et al., Rapid quantification of oxygen tension in blood flow with a fluorine nanoparticle reporter and a novel blood flow-enhanced- saturation-recovery (BESR) sequence, Bone 70 (2013) 176–183.

[36] M.M. Kaneda, S. Caruthers, G.M. Lanza, S.A. Wickline, Perfluorocarbon Nanoemulsions for quantitative molecular imaging and targeted therapeutics, Ann. Biomed. Eng. 37 (2009) 1922–1933.
[37] C. Jacoby, et al., Probing different perfluorocarbons for in vivo inflammation imaging by 19F MRI: image reconstruction, biological half-lives and sensitivity, NMR Biomed. 27 (2014) 261–271.
[38] J. Yu, V. Kodibagkar, W. Cui, R. Mason, 19F: a versatile reporter for non-invasive physiology and pharmacology using magnetic resonance, Curr. Med. Chem. 12 (2005) 819–848.
[39] Z.-X. Jiang, X. Liu, E.-K. Jeong, Y.B. Yu, Symmetry-guided design and Fluorous synthesis of a stable and rapidly excreted imaging tracer for19F MRI, Angew. Chem. Int. Ed. 48 (2009) 4755–4758.
[40] J.M. Janjic, M. Srinivas, D.K.K. Kadayakkara, E.T. Ahrens, Self-delivering nanoemulsions for dual fluorine-19 MRI and fluorescence detection, J. Am. Chem. Soc. 130 (2008) 2832–2841.
[41] R.P. Mason, W. Rodbumrung, P.P. Antich, Hexafluorobenzene: a sensitive 19F NMR indicator of tumor oxygenation, NMR Biomed. 9 (1996) 125–134.
[42] L. Mignion, et al., Hexafluorobenzene in comparison with perfluoro-15-crown-5-ether for repeated monitoring of oxygenation using 19F MRI in a mouse model, Magn. Reson. Med. 69 (2013) 248–254.
[43] R. Schwarz, M. Schuurmans, J. Seelig, B. Künnecke, 19F-MRI of perfluorononane as a novel contrast modality for gastrointestinal imaging, Magn. Reson. Med. 41 (1999) 80–86.
[44] M.H. Cho, et al., Targeted, stimuli-responsive, and Theranostic 19F magnetic resonance imaging probes, Bioconjug. Chem. 30 (2019) 2502–2518.
[45] J.G. Riess, Oxygen carriers ('blood substitutes') - raison d'etre, chemistry, and some physiology, Chem. Rev. 101 (2001) 2797–2919.
[46] M.P. Krafft, J.G. Riess, Chemistry, physical chemistry, and uses of molecular fluorocarbon - hydrocarbon Diblocks, Triblocks, and related compounds, Chem. Rev. 109 (2009) 1714–1792.
[47] E.T. Ahrens, R. Flores, H. Xu, P.A. Morel, In vivo imaging platform for tracking immunotherapeutic cells, Nat. Biotechnol. 23 (2005) 983–987.
[48] M. Srinivas, P.A. Morel, L.A. Ernst, D.H. Laidlaw, E.T. Ahrens, Fluorine-19 MRI for visualization and quantification of cell migration in a diabetes model, Magn. Reson. Med. 58 (2007) 725–734.
[49] D.A. Ingram, M.B. Forman, J.J. Murray, Activation of complement by Fluosol attributable to the pluronic detergent micelle structure, J. Cardiovasc. Pharmacol. 22 (1993) 456–461.
[50] M.S. Fox, J.M. Gaudet, P.J. Foster, Fluorine-19 mri contrast agents for cell tracking and lung imaging, Magn. Reson. Insights 8s1 (2015). MRI.S23559.
[51] L.C. Rose, et al., Fluorine-19 labeling of stromal vascular fraction cells for clinical imaging applications, Stemcells Transl. Med. 4 (2015) 1472–1481.
[52] M.G. Freire, A.M.A. Dias, M.A.Z. Coelho, J.A.P. Coutinho, I.M. Marrucho, Aging mechanisms of perfluorocarbon emulsions using image analysis, J. Colloid Interface Sci. 286 (2005) 224–232.
[53] J.G. Riess, M. Postel, Stability and stabilization of fluorocarbon emulsions destined for injection, Biomater. Artif. Cells Immobil. Biotechnol. 20 (1992) 819–830.
[54] U. Flögel, et al., In Vivo Monitoring of Inflammation After Cardiac and Cerebral Ischemia by 19F Magnetic Resonance Imaging 118, 2009, pp. 140–148.
[55] S. Temme, et al., Noninvasive imaging of early venous thrombosis by19F magnetic resonance imaging with targeted perfluorocarbon nanoemulsions, Circulation 131 (2015) 1405–1414.
[56] M. Srinivas, et al., PLGA-encapsulated perfluorocarbon nanoparticles for simultaneous visualization of distinct cell populations by 19F MRI, Nanomedicine 10 (2015) 2339–2348.
[57] O. Diou, et al., Long-circulating perfluorooctyl bromide nanocapsules for tumor imaging by 19FMRI, Biomaterials 33 (2012) 5593–5602.
[58] T. Boissenot, et al., Paclitaxel-loaded PEGylated nanocapsules of perfluorooctyl bromide as theranostic agents, Eur. J. Pharm. Biopharm. 108 (2016) 136–144.
[59] A. Zielinska, et al., Polymeric nanoparticles: production, characterization, toxicology and ecotoxicology Aleksandra, Molecules 25 (2020) 3731.
[60] B.P. Barnett, et al., Fluorocapsules for improved function, Immunoprotection, and visualization of cellular therapeutics with MR, US, and CT imaging, Radiology 258 (2011) 182–191.
[61] J.V. Jokerst, T. Lobovkina, R.N. Zare, S.S. Gambhir, Nanoparticle PEGylation for imaging and therapy, Nanomedicine 6 (2011) 715–728.
[62] A.L. Klibanov, K. Maruyama, V.P. Torchilin, L. Huang, Amphipathic polyethyleneglycols effectively prolong the circulation time of liposomes, FEBS Lett. 268 (1990) 235–237.
[63] P. Calvo, et al., Long-circulating PEGylated Polycyanoacrylate nanoparticles as new drug carrier for brain delivery, Pharm. Res. 18 (2001) 1157–1162.
[64] L. Nobs, F. Buchegger, R. Gurny, E. Allémann, Surface modification of poly(lactic acid) nanoparticles by covalent attachment of thiol groups by means of three methods, Int. J. Pharm. 250 (2003) 327–337.
[65] K. Abstiens, S. Maslanka Figueroa, M. Gregoritza, A.M. Goepferich, Interaction of functionalized nanoparticles with serum proteins and its impact on colloidal stability and cargo leaching, Soft Matter 15 (2019) 709–720.
[66] R.A. Petros, J.M. Desimone, Strategies in the design of nanoparticles for therapeutic applications, Nat. Rev. Drug Discov. 9 (2010) 615–627.
[67] A. Moreno-Aspitia, E.A. Perez, Nanoparticle albumin-bound paclitaxel (ABI-007): a newer taxane alternative in breast cancer, Future Oncol. 1 (2005) 755–762.
[68] P.K. Bae, et al., Bimodal perfluorocarbon nanoemulsions for nasopharyngeal carcinoma targeting, Mol. Imaging Biol. 15 (2013) 401–410.
[69] C. Giraudeau, et al., 19F molecular MR imaging for detection of brain tumor angiogenesis: in vivo validation using targeted PFOB nanoparticles, Angiogenesis 16 (2013) 171–179.
[70] Y. Zhang, et al., Intratumoral glutathione Activatable Nanoprobes for fluorescence and 19F magnetic resonance turn-on imaging, Anal. Chem. 92 (2020) 15679–15684.
[71] S. Wilhelm, et al., Analysis of nanoparticle delivery to tumours, Nat. Rev. Mater. 1 (2016) 16014.
[72] H. Dewitte, et al., Design and evaluation of theranostic perfluorocarbon particles for simultaneous antigen-loading and 19F-MRI tracking of dendritic cells, J. Control. Release 169 (2013) 141–149.
[73] H. Matsushita, et al., Multifunctional core-shell silica nanoparticles for highly sensitive 19F magnetic resonance imaging, Angew. Chem. Int. Ed. 53 (2014) 1008–1011.
[74] T. Nakamura, et al., Mesoporous silica nanoparticles for 19F magnetic resonance imaging, fluorescence imaging, and drug delivery, Chem. Sci. 6 (2015) 1986–1990.
[75] J. Zhao, et al., Recent developments in multimodality fluorescence imaging probes, Acta Pharm. Sin. B 8 (2018) 320–338.
[76] S. Chen, Y. Yang, H. Li, X. Zhou, M. Liu, pH-Triggered Au-fluorescent mesoporous silica nanoparticles for 19F MR/fluorescent multimodal cancer cellular imaging, Chem. Commun. 50 (2014) 283–285.
[77] I. Ashur, H. Allouche-Arnon, A. Bar-Shir, Calcium fluoride Nanocrystals: tracers for in vivo 19F magnetic resonance imaging, Angew. Chem. Int. Ed. 57 (2018) 7478–7482.
[78] W. Du, et al., Amphiphilic hyperbranched fluoropolymers as nanoscopic 19F magnetic resonance imaging agent assemblies, Biomacromolecules 9 (2008) 2826–2833.
[79] N. Feiner-Gracia, et al., Micellar stability in biological media dictates internalization in living cells, J. Am. Chem. Soc. 139 (2017) 16677–16687.
[80] P. Huang, et al., Fluorine meets amine: reducing microenvironment-induced amino-Activatable Nanoprobes for 19F-magnetic resonance imaging of Biothiols, ACS Appl. Mater. Interfaces 10 (2018) 18532–18542.
[81] K. Wang, H. Peng, K.J. Thurecht, S. Puttick, A.K. Whittaker, PH-responsive star polymer nanoparticles: potential 19F MRI contrast agents for tumour-selective imaging, Polym. Chem. 4 (2013) 4480–4489.
[82] K. Wang, H. Peng, K.J. Thurecht, S. Puttick, A.K. Whittaker, Biodegradable core crosslinked star polymer nanoparticles as 19F MRI contrast agents for selective imaging, Polym. Chem. 5 (2014) 1760–1771.
[83] B.E. Rolfe, et al., Multimodal polymer nanoparticles with combined 19F magnetic resonance and optical detection for tunable, targeted, multimodal imaging in vivo, J. Am. Chem. Soc. 136 (2014) 2413–2419.
[84] M.M. Bailey, S.R. Kline, M.D. Anderson, J.L. Staymates, C. Berkland, Chemically modifiable fluorinated copolymer nanoparticles for 19F-MRI contrast enhancement, J. Appl. Polym. Sci. 116 (2012) 2658–2667.
[85] L. Nurmi, et al., Synthesis and evaluation of partly fluorinated polyelectrolytes as components in 19F MRI-detectable nanoparticles, Polym. Chem. 1 (2010) 1039–1047.
[86] G. Neri, et al., Fluorinated PLGA nanoparticles for enhanced drug encapsulation and 19F NMR detection, Chem. - A Eur. J. 26 (2020) 10057–10063.
[87] M. Ogawa, et al., Fluorinated polymer nanoparticles as a novel 19F MRI contrast agent prepared by dendrimer-initiated living radical polymerization, Macromol. Chem. Phys. 211 (2010) 1369–1376.
[88] M. Ogawa, et al., Synthesis and evaluation of water-soluble fluorinated dendritic block-copolymer nanoparticles as a 19F-MRI contrast agent, Macromol. Chem. Phys. 211 (2010) 1602–1609.
[89] J. Yang, Q. Zhang, H. Chang, Y. Cheng, Surface-engineered Dendrimers in gene delivery, Chem. Rev. 115 (2015) 5274–5300.
[90] J.M. Criscione, et al., Self-assembly of pH-responsive fluorinated dendrimer-based particulates for drug delivery and noninvasive imaging, Biomaterials 30 (2009) 3946–3955.
[91] Q. Xiao, et al., Self-sorting and Coassembly of fluorinated, hydrogenated, and hybrid Janus Dendrimers into Dendrimersomes, J. Am. Chem. Soc. 138 (2016) 12655–12663.
[92] L. Ren, et al., Efficient temperature-feedback liposome for 19F MRI signal enhancement, Chem. Commun. 56 (2020) 14427–14430.
[93] M. Chan, A. Almutairi, Nanogels as imaging agents for modalities spanning the electromagnetic spectrum, Mater. Horizons 3 (2016) 21–40.
[94] M. Oishi, S. Sumitani, Y. Nagasaki, On-off regulation of 19F magnetic resonance signals based on pH-sensitive PEGylated nanogels for potential tumor-specific smart 19F MRI probes, Bioconjug. Chem. 18 (2007) 1379–1382.
[95] O. Munkhbat, et al., 19 F MRI of polymer Nanogels aided by improved segmental mobility of embedded fluorine moieties, Biomacromolecules 20 (2019) 790–800.
[96] K. Kolouchova, et al., Self-assembled Thermoresponsive polymeric Nanogels for 19F MR imaging, Biomacromolecules 19 (2018) 3515–3524.
[97] D. Babuka, et al., Internal structure of thermoresponsive physically crosslinked nanogel of poly[N-(2-hydroxypropyl) methacrylamide]-block-poly[N-(2,2-difluoroethyl) acrylamide], prominent 19 F MRI tracer, Nanomaterials 10 (2020) 1–17.
[98] A.T. Preslar, et al., Calcium-induced morphological transitions in peptide Amphiphiles detected by 19F-magnetic resonance imaging, ACS Appl. Mater. Interfaces 9 (2017) 39890–39894.
[99] K.L. Peterson, K. Srivastava, V.C. Pierre, Fluorinated paramagnetic complexes: sensitive and responsive probes for magnetic resonance spectroscopy and imaging, Front. Chem. 6 (2018) 1–21.

[100] P. Harvey, I. Kuprov, D. Parker, Lanthanide complexes as paramagnetic probes for 19F magnetic resonance, Eur. J. Inorg. Chem. 2012 (2015–2022), https://doi.org/10.1002/ejic.201100894.
[101] K.H. Chalmers, A.M. Kenwright, D. Parker, A.M. Blamire, 19F-Lanthanide Complexes With Increased Sensitivity for F-MRI: Optimization of the MR Acquisition 936, 2011, pp. 931–936.
[102] A.M. Neubauer, et al., Gadolinium-modulated 19F signals from perfluorocarbon nanoparticles as a new strategy for molecular imaging, Magn. Reson. Med. 60 (2008) 1066–1072.
[103] M.B. Kok, et al., Quantitative 1H MRI, 19F MRI, and 19F MRS of cell-internalized perfluorocarbon paramagnetic nanoparticles, Contrast Media Mol. Imaging 6 (2011) 19–27.
[104] A.M. Morawski, et al., Quantitative 'magnetic resonance immunohistochemistry' with ligand-targeted 19F nanoparticles, Magn. Reson. Med. 52 (2004) 1255–1262.
[105] T. Nakamura, et al., Activatable 19F MRI nanoparticle probes for the detection of reducing environments, Angew. Chem. Int. Ed. 54 (2015) 1007–1010.
[106] K. Akazawa, F. Sugihara, T. Nakamura, S. Mizukami, K. Kikuchi, Highly sensitive detection of Caspase-3/7 activity in living mice using enzyme-responsive 19 F MRI Nanoprobes, Bioconjug. Chem. 29 (2018) 1720–1728.
[107] Z. Huang, et al., A fluorinated dendrimer-based nanotechnology platform: new contrast agents for high field imaging, Investig. Radiol. 45 (2010) 641–654.
[108] A.A. Kislukhin, et al., Paramagnetic fluorinated nanoemulsions for sensitive cellular fluorine-19 magnetic resonance imaging, Nat. Mater. 15 (2016) 662–668.
[109] Q. Peng, et al., Paramagnetic nanoemulsions with unified signals for sensitive 19F MRI cell tracking, Chem. Commun. 54 (2018) 6000–6003.
[110] A. Kimura, M. Narazaki, Y. Kanazawa, H. Fujiwara, 19F magnetic resonance imaging of perfluorooctanoic acid encapsulated in liposome for biodistribution measurement, Magn. Reson. Imaging 22 (2004) 855–860.
[111] M. Srinivas, P. Boehm-Sturm, C.G. Figdor, I.J. de Vries, M. Hoehn, Labeling cells for in vivo tracking using 19F MRI, Biomaterials 33 (2012) 8830–8840.
[112] L. Wu, et al., Perfluorocarbons-based 19F magnetic resonance imaging in biomedicine, Int. J. Nanomedicine 15 (2020) 7377–7395.
[113] O. Koshkina, et al., Multicore liquid Perfluorocarbon-loaded multimodal nanoparticles for stable ultrasound and 19 F MRI applied to in vivo cell tracking, Adv. Funct. Mater. 29 (2019) 1–14.
[114] A.H.J. Staal, et al., In vivo clearance of 19F MRI imaging nanocarriers is strongly influenced by nanoparticle ultrastructure, Biomaterials 261 (2020).
[115] D.K.K. Kadayakkara, J.M. Janjic, L.K. Pusateri, W. Bin Young, E.T. Ahrens, In vivo observation of intracellular oximetry in perfluorocarbon-labeled glioma cells and chemotherapeutic response in the CNS using fluorine-19 MRI, Magn. Reson. Med. 64 (2010) 1252–1259.
[116] F. Bonetto, et al., A novel 19 F agent for detection and quantification of human dendritic cells using magnetic resonance imaging, Int. J. Cancer 129 (2011) 365–373.